

HARL TM-26

AD No. 34779

ASTIA FILE COPY

OFFICE OF NAVAL RESEARCH  
CONTRACT N5 ORI-76 PROJECT ORDER X

NR-384-903

CFA  
PAR  
CHU

TECHNICAL MEMORANDUM  
NO. 26

PROPERTY OF R.D.  
TECHNICAL LIBRARY

GASEOUS-TYPE CAVITATION IN LIQUIDS

BY

MURRAY D. ROSENBERG

AUGUST 1, 1953

---

---

ACOUSTICS RESEARCH LABORATORY  
DIVISION OF APPLIED SCIENCE  
HARVARD UNIVERSITY-CAMBRIDGE, MASSACHUSETTS

THIS REPORT HAS BEEN DELIMITED  
AND CLEARED FOR PUBLIC RELEASE  
UNDER DOD DIRECTIVE 5200.20 AND  
NO RESTRICTIONS ARE IMPOSED UPON  
ITS USE AND DISCLOSURE,

DISTRIBUTION STATEMENT A

APPROVED FOR PUBLIC RELEASE;  
DISTRIBUTION UNLIMITED,

Office of Naval Research  
Contract N6ori-76, Project Order X

---

Technical Memorandum 26  
Gaseous-Type Cavitation in Liquids

by

Murray D. Rosenberg

August 1, 1953

Summary

Experimental data are presented regarding the production and growth of gaseous-type (air-filled) bubbles by means of ultrasonic waves in liquids of different physical properties. Evidence is shown that the most logical sources of cavitation nuclei are foreign surfaces within the liquid, either colloidal (dust) particles or parts of the physical apparatus. Experimental apparatus is described for the focusing of sound waves, and the insertion and agitation of pure liquids in thin-walled flasks at the focus. The threshold for gaseous-type cavitation is measured as a function of viscosity, pulse length, and ambient hydrostatic pressure. Finally a comparison between theoretical calculations and experimental results is presented.

---

Acoustics Research Laboratory  
Division of Applied Science  
Harvard University  
Cambridge, Massachusetts

#### PREFACE

In Technical Memorandum No. 25 a theoretical discussion regarding the growth of gas-filled bubbles in a sound field was presented. This memorandum is based upon an experimental study of the growth mechanism and is, therefore, closely related to its predecessor.

## C O N T E N T S

	Page
Preface	
I. Introduction	1
II. Cavitation Nuclei	
(a) Introduction	3
(b) Kinetic theory	4
(c) Suspended particles and surface effects	5
(d) The microscopic examination of liquids	15
(e) Surface tension and other properties	17
III. The Experimental Apparatus	
(a) The mechanical apparatus	19
(b) The diffraction of sound by the paraboloidal mirror	24
(c) The electronic apparatus	28
(d) Preparation of flask and liquids to be tested	31
(e) The saturation of gases in liquids	33
IV. Experimental Results	
(a) Description of gaseous-type cavitation	36
(b) First and second order forces on gas-filled bubbles	40
(c) A tabulation of the physical properties of the liquids examined	45
(d) The quantitative results	47
(e) Some qualitative conclusions regarding gaseous-type cavitation	50
V. Comparison between Theory and Experiment	
(a) The threshold for rectified diffusion	51
(b) Summary	60
VI. Epilogue	60
Bibliography	62

## GASEOUS-TYPE CAVITATION IN LIQUIDS

by

Murray D. Rosenberg

Acoustics Research Laboratory

Harvard University, Cambridge, Massachusetts

### I.

#### INTRODUCTION

The term "cavitation" (see Parsons and Cook[1])\* originally referred to the damage and erosion of surfaces caused by the collapse of cavities in liquids. Wislicenus [2] has properly suggested that the term "cavitation erosion" should be applied to the above process while the word "cavitation" should be defined as the formation and collapse of gas-filled or vapor-filled cavities in a liquid. These cavities are formed by a local reduction of pressure in the liquid under consideration. They subsequently collapse with increased pressure.

Inasmuch as this phenomenon is commonly encountered in many scientific fields, interest in cavitation has been extensive during the past century. Mechanical and hydraulic engineers are concerned with the prevention of cavitation erosion and possible corrosion in the design of turbines, propellers, underwater missiles, and similar structures. Biologists and physiologists are seeking more knowledge concerning the tensile strength of liquids such as tree sap, and the formation of gas bubbles in the bloodstream. And finally, the physicist and acoustical engineer must cope with the cavitation problem when working with underwater transducers, cavitation noise, and the propagation of acoustical signals through media in which cavitation is occurring.

In the past few years several excellent bibliographies have been published regarding cavitation and are listed in references [3-8]. A study of these extensive references indicates not only the elaborate research

- - - - -  
\*References to articles included in the Bibliography are made by numbers enclosed in brackets, [ ].

which has already been accomplished, but also the necessity for filling certain large gaps in this research. In fact, the results of the many investigations of the cavitation problem often vary by factors of a hundred or more. This great disparity has been charged to several effects such as the presence of foreign particles, microscopic gaseous nuclei, and all manner of surface phenomena. Hence, it is extremely difficult to develop a consistent relationship between theory and experiment.

The common forms of cavitation bubbles can be divided into various classes: (a) those whose growth is principally dependent upon the accumulation of several smaller bubbles; (b) those primarily developed by a simple and unidirectional diffusion of dissolved gases that come out of solution (commonly referred to as the degassing of a liquid); (c) those primarily developed by a net influx or rectified diffusion of gas resulting from an alternating influx and efflux of gas across the surface of the bubble (which we shall denote as gaseous-type cavitation bubbles); (d) those developed by sudden decreases in pressure leading to bubbles principally composed of vapor and called vaporous-type cavitation bubbles; and (e) various combinations of the above forms. Collapse or reduction in size of the bubbles will take place with an increase in pressure. The differences and similarities of the two forms of cavitation bubbles have not always been noted in the literature. Experimental observations on bubbles assumed to be vapor-filled have been questioned by other experimenters. As an example, Briggs, Johnson, and Mason [9] describe experiments on vapor-filled cavities in "degassed" liquids while Blake [3] notes that their description applies to gas-filled cavities. Most of the theoretical work in cavitation has been related to vapor-filled cavities. This greater interest is due to the fact that cavitation erosion and its corresponding effect in reducing the efficiency of hydraulic systems is principally the result of the violent and uncushioned collapse of vapor-filled cavities. Thus, only a limited amount of research has been conducted with regard to "gaseous-type cavitation."

The purpose of this study has been to observe experimentally the onset of cavitation in air-saturated liquids of different physical properties, and to develop a theory regarding the growth and collapse of gas-filled bubbles. As will be seen in later chapters, this study leads

to more information regarding cavitation nuclei in liquids; the manner in which gases entrain and dissolve in liquids; and the process by which gas-filled cavitation bubbles are formed. It is hoped that this knowledge might eventually be used in practical engineering applications such as the cushioning of the intense collapse of vapor-filled cavities, or the increased efficiency of ultrasonic signalling devices in sea water.

The apparatus used in the experiment is designed to allow for the production of cavitation by means of an ultrasonic signal in the body of the liquid in order to avoid surface effects. The ultrasonic signal is focused by a paraboloidal reflector so as to accomplish this process. In addition, the apparatus has been designed so as to prevent supersaturation or undersaturation of air in the liquid to be tested. Gas-saturated solutions are obtained by means of mechanical agitation of the liquid. The equipment and the experimental procedures adopted are described in the central sections of this paper. The initial chapter is devoted to a careful study of cavitation nuclei. The final chapters present an analysis regarding the experimental results and the theory of gaseous nuclei and rectified diffusion.

## II.

### CAVITATION NUCLEI

#### A. Introduction.

The extreme variability of the cohesive pressure of a liquid has resulted in the development of numerous theoretical devices in order to explain the experimental results. Calculations regarding the intrinsic tensile strength of a liquid that are based upon van der Waal's Law predict values that are many orders of magnitude higher than the observed values. For example, in van der Waal's equation,

$$(p + \frac{a}{v^2}) (v - b) = R * T$$

the term  $a/v^2$  represents the effect of intermolecular attractions or an intrinsic pressure. For the case of water at S. T. P., this intrinsic pressure is approximately 10,000 atmospheres, a value far in excess of the 1 to 200 atmospheres that have been observed. Other manipulations of the van der Waal's equation predict tensile strengths of approximately 600

atmospheres, a more reasonable figure, but still far out of agreement with experimental data. References regarding the use of the van der Waal's equation for predicting the tensile strength of liquids can be found in the elaborate work of Temperley and Chambers [10] and of Benson and Gerjuoy [11]. However, it is apparent that recourse must be made to some other principles in order to formulate a theoretical basis for the tensile strength of a liquid.

Present experimental data on liquids indicates that the static or intrinsic liquid cohesive pressure has been relieved by the formation of a vapor or gas-vapor bubble of small size. This small bubble then serves as the weak point in the liquid or, in the case of cavitation, as the cavitation nucleus. The purpose of this chapter is to examine the manner in which these nuclei become present in the liquid.

#### B. Kinetic theory.

The kinetic theory of liquids is intimately involved with the physical model chosen to represent the liquid state of matter. Current investigators tend to look upon the liquid state of matter as a pseudo-crystalline structure (at not too high temperatures) in which there exists a large number of vacant lattice sites resulting in the fluidity of the model. The existence of these vacant sites or holes indicates that they might serve as the cavitation nuclei within the liquid. A discussion of the kinetic theory of holes in liquids or the kinetics of phase transitions is not within the scope of this paper. Usually the average energy of hole formation is determined on the basis of the Maxwell-Boltzmann distribution law, and the average hole size is then calculated. This method only applies to systems in statistical equilibrium. Since a superheated liquid, or one under tension is in a metastable state, Doring [12] and Volmer [13] calculated the rate of formation of holes of critical size in accordance with the relative rates of condensation and evaporation. Other researchers (e. g., Fisher [14] and Turnbull and Fisher [15]) have applied the theory of chemical reaction rates to determine the rate of formation of these critical nuclei. For a complete presentation of these methods one is referred to the books of Frenkel [16] and Volmer [13]; the short bibliography and outline of Blake [3]; and the more recent articles of Born and Green [7]. Regardless of the theoretical method adopted, these

references show that the holes in a liquid in statistical equilibrium will not be appreciably greater than  $10^{-8}$  cm in radius. Nor will these holes develop to a sufficiently large nucleus in a reasonable amount of time unless, in the case of water, for example, a tension of approximately 4000 atmospheres is applied.

One may be tempted to apply Fermi-Dirac or Bose-Einstein statistics to the above problem. However, both of these forms of statistics will not differ appreciably from the classical Maxwellian if the number of holes per unit volume is not large [18], [19]. Define the quantity  $n/v$  as the density of monomolecular vapor bubbles. According to the treatment of Doring, [12], the molecular heat of vaporization is required for the production of a hole in a liquid. Then

$$\frac{n}{v} = N_1 e^{-\frac{\lambda}{kt}},$$

where

$N_1$  = density of fluid molecules

$\lambda$  = latent molecular heat of vaporization

$k$  = Boltzmann's constant

One can show that the density of holes in water is a negligible order of magnitude unless the liquid is heated to a temperature in the vicinity of its critical point. It is, therefore, apparent that some other line of reasoning must be adopted to bring about a closer agreement between theory and experiment.

#### C. Suspended particles and surface effects.

It has long been noted by several experimenters, for example, Dean [20], Cassel [21], Harvey et al [22], that the presence of a particle or wall surface in a liquid will lessen the ability of a liquid to undergo superheating, supersaturation, or tensile stresses. The effect of the surface is in no way dependent on its geometry, but rather on its ability to adsorb gases and/or on its affinity for the liquid in question (that is, whether it is lyophobic or lyophilic). It is, therefore, useful to review the physical principles involved in the phenomena exhibited by surfaces. An excellent discussion of interfaces and surfaces is given in a book by Bikerman [23] that also provides a very extensive bibliography.

The most amazing property of all surfaces is their surface tension or free surface energy. For liquid-gas surfaces the surface tension can be defined as the force per unit length that acts along the surface and tends to make its area a minimum. Similarly, the free surface energy is simply the energy that must be expended to increase the surface by a unit area at constant temperature, and that would be then stored in the surface. The most striking manifestation of surface energy is the additional pressure that occurs under the concave side of curved surfaces. This additional or capillary pressure is a function of the surface tension,  $\sigma$ , and the curvature of the surface. For a curved surface that can be described geometrically by two principal radii of curvature the capillary pressure,  $p_c$ , is

$$p_c = \sigma \left( \frac{1}{R'} + \frac{1}{R''} \right)$$

where  $R'$  and  $R''$  are the main radii of curvature for a given point on the surface. For a spherical bubble this equation reduces to

$$p_c = \frac{2\sigma}{R} .$$

The problem of wetting involves three phases, the solid, the liquid, and the gas. The forces between the molecules of the liquid are called cohesive forces. The forces between the liquid molecules and those of the solid are called adhesive forces. As a result of the interplay of molecular forces, a contact angle will be established at the point common to the three phases as shown in Fig. 1.

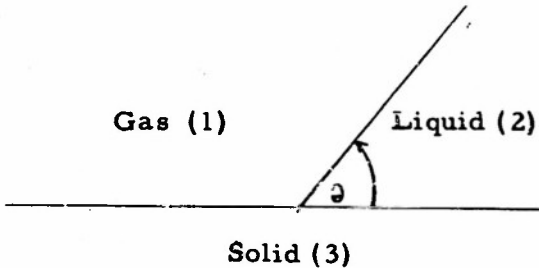


Fig. 1.

For a flat solid enclosing an angle of  $180^\circ$ , the angle within the liquid is denoted by  $\theta$ , the contact angle. Define  $\sigma_{13}$  as the surface tension of the solid in contact with the gaseous phase;  $\sigma_{12}$  as the surface tension of the liquid in contact with the gaseous phase; and  $\sigma_{23}$  as the interfacial tension between the solid and the liquid. If the gaseous phase is made up of an "inactive gas" saturated with vapor,  $\sigma_{13}$  and  $\sigma_{12}$  are simply the surface tensions of the solid and liquid respectively. Assuming that this three-phase contact is in equilibrium

$$\sigma_{13} - \sigma_{23} = \sigma_{12} \cos \theta.$$

The work that must be done to separate a unit area of the liquid from the solid wall is

$$W_a = \sigma_{13} + \sigma_{12} - \sigma_{23},$$

and is called the free energy of adhesion. The work required to separate one unit area of the liquid from another unit area of the liquid is

$$W_c = 2\sigma_{12},$$

and is called the free energy of cohesion. Inasmuch as  $\sigma_{13}$  and  $\sigma_{23}$  are not readily known, one can write in terms of the contact angle that

$$W_a = \sigma_{12} (1 + \cos \theta).$$

In general  $W_a < W_c$ , and the liquid is more easily separated from a solid than itself. Theoretically  $W_a$  can be greater than  $W_c$ , or for cases of perfect non-wetting  $W_a$  can be less than or equal to zero. Blake [3], however, has shown that there is no experimental evidence for the existence of a contact angle closely approaching  $180^\circ$ . In addition, he has shown that the energy of bubble formation on a plane or even convex surface will be reduced by an appreciable amount only if  $\theta$  is within a few degrees of  $180^\circ$ . Thus it appears unreasonable that the wettability or lack of adhesion of the liquid to a "smooth" solid particle provides the proper explanation regarding the existence of cavitation nuclei of proper size. Similar remarks hold for convex surfaces.

Although the wetting of plane or convex surfaces is unfavorable to the formation of a nucleus of sufficient radius, the wetting of a concave surface or wall crack is most favorable. From the point of view of de novo

formation, Harvey [24] has stated that thermal energy fluctuations are sufficient to result in the formation of a gas-filled or vapor-filled cell at the apex angle,  $2\alpha$ , of a conical crack provided that the receding contact angle of the liquid is  $\theta_R > \frac{\pi}{2} + \alpha$ . Although Harvey does not provide the mathematical derivation for this equation, one can readily show by means of the geometry of the bubble that the ratio of the energy of formation for a bubble within a conical crack to the energy of formation for a spherical bubble of the same radius of curvature is

$$\Theta(\alpha, \theta_R) = \frac{1}{4} \left[ \frac{\cos^2(\alpha - \theta_R) \cos \theta_R}{\sin \alpha} + 2 \sin(\alpha - \theta_R) + 2 \right]$$

When  $\theta_R \geq \frac{\pi}{2} + \alpha$ ,  $\Theta(\alpha, \theta_R) \leq 0$ , and the de novo formation of a bubble in a conical crack can occur. When  $\alpha = \frac{\pi}{2}$ ,  $\Theta(\alpha, \theta_R) = \frac{1}{4} [2 + 3 \cos \theta_R - \cos^3 \theta_R]$ , which is the ratio one obtains for the case of bubble formation on a plane surface. In this case de novo bubble formation will not occur unless  $\theta_R \approx 180^\circ$ , a physical value that has not yet been observed.

Hence thermal energy fluctuations can initiate the formation of a bubble within a crack if  $\theta_R \geq \frac{\pi}{2} + \alpha$ . Since an external gas-saturated liquid will be supersaturated with respect to the bubble, gas will diffuse into the bubble until a stable condition is reached. At equilibrium, the geometry of the crack and the contact angle will be such that the capillary pressure effects ( $P_C = \sigma \left( \frac{1}{R} + \frac{1}{R'} \right)$ ) are negligible for the case of a saturated gas solution, or negative (that is, negative radii of curvature are possible) for the unsaturated gas solution.

A second possibility regarding sources for cavitation nuclei is that there is stabilized within cracks a residual amount of gas that resists going into solution even if the external liquid has been conventionally degassed. This residual gas can be stabilized as a result of the adhesion between molecules of the gas and the surface molecules of the solid; that is, the adsorptive process. In addition, imperfectly wetted cracks, variations in advancing and receding contact angles, and the surface geometry of the liquid surface will assist in stabilizing the gas in the crack.

The experimental evidence of Harvey [25] and Blake [3] indicates that both sources of cavitation nuclei probably occur in cracks; that is, the de novo formation and the presence of small amounts of residual gas.

Hence, in a gas-saturated liquid a source for a cavitation nucleus may consist of a conical crack that is partially filled with gas. The question that must now be answered is how this crack finally provides a cavitation nucleus of radius,  $R_0$ .

In all probability, the manner in which a gas-filled crack serves as a source for a cavitation nucleus of suitable size is extremely complicated. However, various phases of the mechanism can be described. It will be shown that  $R_0$  must be of the order of magnitude of  $10^{-4}$  to  $10^{-5}$  cm. The existence of surface cracks with mouth diameters of approximately  $10^{-5}$  cm necessitates the presence of a wall surface or suspended particles approximately  $10^{-4}$  cm in diameter whose surface roughness can then supply the required concave cracks. The presence of a wall surface depends upon the design of the experiment. Fine particles, however, are practically always available for the contamination of liquids. Dalla Valla [26] has shown that the mean size of atmospheric dust is roughly 0.5 microns while the mean size of industrial dust is slightly greater than one micron. Numerous experimenters have noted the presence of particles or "motes" in liquids and the extreme difficulty in removing them. Dean [20] prepared a mote-free lanolin solution but found that a momentary exposure of the solution to air greatly replenished the supply of motes. It appears, therefore, that the sources for the cavitation nuclei in liquids that are free of wall surfaces and that have not been specially treated, consist chiefly of dust particles ranging from  $5 \times 10^{-5}$  to  $10^{-3}$  cm in diameter with a surface roughness that allows for cracks with a mean diameter varying between  $10^{-6}$  cm and  $10^{-5}$  cm. Although it is extremely difficult to obtain experimental evidence regarding the submicroscopic roughness of surfaces, evidence presented by Bikerman (pp. 169-179, [23]) shows that interferometer and electron microscope measurements indicate the presence of surface roughness of this order of magnitude.

With the application of an acoustical signal the liquid surface within the crevice will oscillate. If the acoustical signal is of large enough amplitude, a net amount of gas will diffuse into the gas volume within the crevice. After a sufficient number of cycles, a growing bubble can issue forth from the cavity and serve as the cavitation nucleus.

Prior to the establishment of this situation certain requirements must be satisfied so that the surface between the gas and the liquid within the crack will move outward. Because of the complicated geometry of the crack and changes in contact angle, the relations that determine the condition for the outward movement of this surface as a result of diffusion will differ considerably from those for a free spherical gas bubble. In general the minimum peak acoustic pressure,  $A'_{\infty}$ , that is necessary to insure the outward movement of the liquid surface will be less than the minimum peak acoustic pressure,  $A_{\infty}$ , required for the growth (through diffusion) of a spherical bubble of radius  $R_0$  (see reference [27]). The value of  $A'_{\infty}$  can be estimated in the following manner. The number of gas mols crossing the surface,  $S$ , in unit time is

$$m = S D a \frac{\partial p}{\partial r} \Big|_{sfc},$$

where

$a$  = solubility constant

$\frac{\partial p}{\partial r} \Big|_{sfc}$  = pressure gradient across the surface.

Suppose that the surface area  $S$  is proportional to  $(V - V')^{2/3}$ , where  $V$  is the gas volume, and  $V'$  is some constant volume such that  $S$  is zero when  $V=V'$ . That is, assume that the geometry of the crack and variation in contact angle are such that the surface area for diffusion becomes negligible on the positive cycle of the applied sound signal. Assuming that  $V$  is proportional to  $r^3$ , and  $V'$  to  $r_{\min}^3$ , where  $r$  is the radius of curvature of the surface, and  $r_{\min}$  is the minimum value of  $r$ , one can write that

$$m \propto \frac{(r^3 - r_{\min}^3)^{2/3}}{r} (g - P_e - \frac{2\pi}{r}).$$

Using the expansion

$$(r^3 - r_{\min}^3)^{2/3} = r^2 - \frac{2}{3} \frac{r_{\min}^3}{r} + \frac{1}{9} \frac{r_{\min}^6}{r^4} \dots,$$

it follows that

$$m \propto \frac{r^2 - \frac{2}{3} \frac{r_{\min}^3}{r}}{r} (g - P_e - \frac{2\pi}{r}).$$

For a saturated gas solution

$$g - p_e = -A \sin \omega t.$$

The assumption that

$$r \approx r_0(1-a_1 A \sin \omega t), \text{ and } r_{\min} \approx \frac{4}{5} r_0$$

leads to the expression

$$\dot{m} \propto [r_0(1-a_1 A \sin \omega t) - \frac{2}{3} \cdot \frac{4}{5} r_0 (1+2a_1 A \sin \omega t + a_1^2 A^2 \sin^2 \omega t)]$$

$$\cdot [-A(1+a_1 \frac{2\sigma}{r_0}) \sin \omega t - \frac{2\sigma}{r_0}] ,$$

where  $r_0$  is the equilibrium value of  $r$ .

The average value of  $\dot{m}$  over one cycle is

$$\bar{m} \propto [\frac{a_1}{2} (1+a_1 \frac{2\sigma}{r_0}) + \frac{8}{15} a_1 (1+a_1 \frac{2\sigma}{r_0}) + \frac{8}{15} \frac{\sigma}{r_0} a_1^2] A^2 - \frac{2\sigma}{r_0} + \frac{16}{15} \frac{\sigma}{r_0} .$$

The threshold  $A'_{\infty}$  is given by  $\bar{m} = 0$ , or

$$A'_{\infty} = \sqrt{\frac{\frac{4\sigma}{r_0} - \frac{32}{15} \frac{\sigma}{r_0}}{a_1 (1+a_1 \frac{2\sigma}{r_0}) + \frac{16}{15} a_1 (1+a_1 \frac{2\sigma}{r_0}) + \frac{16}{15} \frac{\sigma}{r_0} a_1^2}} .$$

We find in reference [27] that under the same situation the threshold,  $A_{\infty}$ , for a free spherical bubble is given approximately by

$$A_{\infty} = \sqrt{\frac{\frac{4\sigma}{R_0}}{a_1 (1+a_1 \frac{2\sigma}{R_0})}} .$$

Obviously,  $A'_{\infty} \ll A_{\infty}$ , and a peak acoustic pressure less than the threshold for gaseous cavitation will be sufficient to cause an outward movement of the liquid surface within the crevice.

One could speculate indefinitely on the many ways in which small crevices could serve as sources for cavitation nuclei. The principal point,

however, upon which strong emphasis has been placed in the preceding paragraphs is that a very small acoustic signal will in a few cycles (perhaps one cycle is sufficient) result in the outward movement of the liquid surface within a crevice. Following this movement a spherical bubble of radius  $R_0$ , will be initiated within the liquid. The  $A'_\infty$  required to do this will be a small value that is practically the same for all liquids. As will be shown in the following pages, the contact angle between the liquid and the surface of the crack is in all probability approximately 90 degrees. The bubble will probably be free in the liquid once it has issued forth from the cavity or crevice. The final peak acoustic pressure required for the growth of the bubble by means of gaseous diffusion is  $A_\infty$ , whose values will be discussed. This bubble of radius,  $R_0$ , will be referred to as the cavitation nucleus. Its final size will be a function of the amount of gas that can diffuse into it during its formation, and this amount will be a function of the transient variations of the bubble radius as well as the diffusion parameters. The fact that the transient variations of the bubble radius may be much greater than the steady-state variations can be seen from the following simplified analysis.

It has been shown in reference [27] that the impedance, (the ratio of the steady-state incident sound pressure to the velocity of the surface of the bubble), presented by a small bubble of radius,  $R$ , ( $\frac{\omega R}{c} \ll 1$ ) to a sinusoidal pressure wave is approximately

$$Z = \frac{4u}{R} + i \left( \omega \rho R - \frac{1}{\omega \frac{2\sigma}{R}} \right).$$

$$\frac{3(P_o + \frac{2\sigma}{R})}{3(P_o + \frac{2\sigma}{R})}$$

The transient of the bubble pulsation will depend upon the ratio of the damping constant to the undamped angular velocity, namely,

$$\frac{4u}{2\rho R^2} \sqrt{\left( \frac{3(P_o + \frac{2\sigma}{R})}{\rho R^2} \right)^{1/2}} = \frac{2}{\sqrt{3}} \frac{u}{\left[ \rho R (R P_o + 2\sigma) \right]^{1/2}} = g.$$

For a bubble of radius  $R_0 = 10^{-4}$ ,

$$g \approx \frac{u}{\sqrt{2} \times 10^{-1}}$$

For the so called "non-viscous" liquids,  $g \leq 1$ , and an underdamped or oscillatory condition prevails wherein a high frequency transient of rather large magnitude will be superimposed on the steady-state pulsations if the applied signal has the proper phase. For the more viscous liquids, or if  $R_o$  is smaller,  $g \geq 1$ , and a critically damped or overdamped condition results, whereby the transient may still be of rather large magnitude but non-oscillatory. The size of the nucleus,  $R_o$ , will be determined by the amount of gas that can diffuse into the embryonic nucleus during this transient period. This process will be substantiated in chapter V.

Before leaving this subject, one should consider some additional evidence regarding the stabilization of gas within crevices. Briggs, Mason, and Johnson [9] note that a liquid which has once been "poisoned" by cavitation may require up to several hours to regain its strength. This observation will be confirmed; that is, a liquid has a "recovery time." In addition to these observations, Harvey [28] reported that he was able to raise the tensile strength of water by subjecting it to a pressure of 1000 atmospheres for a period of 15 to 30 minutes. It appears that the effect of pressurizing is to force into solution the gas that is stabilized within small cracks.

A theoretical calculation as to the pressurization time of a liquid can be made on the basis of the diffusion equation.

Consider first the rate at which gas will diffuse out of a bubble in a cylindrical crevice. The number of moles leaving per unit area in unit time is proportional to the exposed surface area, and is

$$\dot{m} = \frac{2\pi r}{\cos \theta_A} (1 - \sin \theta_A) a D (g - p_e - \frac{2\sigma}{r} \cos \theta_A)$$

where

$r$  = radius of the capillary

$a$  = solubility constant

$D$  = diffusion coefficient

$\theta_A$  = contact angle (advancing).

In accordance with the perfect gas law

$$(p_e + \frac{2\sigma}{r} \cos \theta_A) (\pi r^2 l + \frac{\pi}{3} \frac{r^3}{\cos^3 \theta_A} (2 - 3 \sin \theta_A + \sin^3 \theta_A)) = m R * T$$

whereby

$$\dot{m} = \frac{\pi r^2 i}{R T} (p_e + \frac{2\sigma}{r} \cos \theta_A),$$

where

$l$  = depth of gas bubble at time  $t$  in crevice of length  $l_0$ .

By equating the two expressions for  $\dot{m}$ , and assuming that  $g = P_o$ ,  $p_e = 1000P_o$ , one obtains

$$i = - \frac{2R * TaD(l - \sin \theta_A) * 999P_o + \frac{2\sigma}{r} \cos \theta_A}{r \cos \theta_A (1000 P_o + \frac{2\sigma}{r} \cos \theta_A)}$$

The time required to fill the crevice completely is approximately,

$$T \approx \frac{r l_0 \cos \theta_A}{2R * TaD(l - \sin \theta_A)}$$

If  $\theta_A = 0$ , that is, for the case of perfect wetting

$$T_{\theta_A=0^\circ} \approx \frac{rl_0}{2R * TaD}$$

For water subject to atmospheric pressure at room temperature, assume that  $r \approx 10^{-5}$  cm, and  $l_0 = 5 \times 10^{-5}$  cm. Then

$$T_{\theta_A=0^\circ} \approx 0.6 \text{ milliseconds.}$$

As  $\theta_A$  approaches  $90^\circ$  the time  $T$  approaches infinity. Thus, if  $\theta_A$  is approximately  $90^\circ$ , a finite amount of time will be required for gas bubbles within crevices to be reabsorbed into solution even though the liquid is subject to a high hydrostatic pressure. Using Harvey's value of 15 minutes of pressurizing, one can easily compute that the advancing contact angle is  $\theta_A = 90^\circ$ . This technique of analysis can obviously be applied to many shapes of cracks or crevices. Little additional speculation is useful unless some exact experimental data becomes available as to the rate and manner in which gases stabilize within crevices.

Before leaving this subject, however, it is advantageous to consider the role played by viscosity in the above process. The empirical equation of Poiseuille [29], later derived by Lamb (p. 584, [30]) states that the movement of a liquid in a cylindrical capillary will be in accordance with the equation,

$$\frac{dh}{dt} = \frac{\pi^2}{8\mu} \frac{\Delta P}{h}$$

where

$\frac{dh}{dt}$  = average velocity in the liquid

$\mu$  = viscosity of the liquid

r = the radius of the capillary

h = the length of the liquid column in the capillary at time t

$\Delta P$  = pressure difference.

The pressure difference is  $(p_e + \frac{2\sigma}{r} \cos \theta - p_g)$ , where  $p_g$  is the pressure of the gas within the crevice. Initially the pressure inside the cavity will be  $p_g = g = P_0$ , and taking  $p_e = 10^3 P_0$  it follows that

$$\frac{1}{2} h^2 = \frac{\pi^2}{8\mu} (999P_0 + \frac{2\sigma}{r} \cos \theta)t,$$

or

$$t = \frac{4\mu l^2}{r(999P_0 + \frac{2\sigma}{r} \cos \theta)}.$$

Using the same values as before and taking any value for  $\theta$ , one obtains the solution that  $t \approx 0.1$  microseconds. Thus, the initial movement of the liquid surface will be extremely rapid and proportional to the viscosity of the liquid. The gas pressure will build up almost immediately to the external pressure such that  $\Delta P = 0$ . The inward movement of the liquid surface will then be controlled by the diffusion process (whose principal controlling parameter is the advancing contact angle). As previously indicated it is then necessary to apply high pressures for a considerable period of time in order to force the gas within the crevice into solution.

#### D. The microscopic examination of liquids.

Colloidal particles with diameters of approximately 1 micron should certainly be observable by means of microscopic or ultramicroscopic techniques [31], [32]. To test this assumption all of the liquids studied in this experiment were subjected to ultramicroscopic examination. The equipment used consisted of a Bausch and Lamb research microscope modified for dark field illumination. The top element of an achromatic 1.40 N. A. substage condenser was removed to give a 0.59 N. A. An achromatic

(16 mm, 10 x 0.25 N.A.) objective was used in conjunction with a compensating single 7.5 x eyepiece in order to observe a wide field. To obtain dark field illumination a dark field stop together with a blue glass moderating disk were inserted in the lower focal plane of the substage condenser. The liquid to be observed was placed on a culture microscope slide with a single depression. The depression in this glass slide is spherical with a diameter of approximately 16.5 mm and a depth of approximately 0.8 mm. The thickness of the slide is about 1.5 mm. A one inch square cover glass (no. 2, 0.17 to 0.25 mm in thickness) was then placed over the liquid. Trial and error techniques must be used to adjust the condenser and objective so as to obtain a maximum amount of contrast between the light reflected by the particles and the dark field. To obtain photographs of the microscopic field, a standard plate camera was mounted on the microscope, and several time exposure pictures at various stops were taken of each liquid. To minimize the effects of Brownian motion by using the shortest amount of time exposure required for good photographs, a fast film (Kodak super panchro-press, type B) was used. In all cases the depression slide and cover glass used were new, never having been used for previous microscopic observations. Prior to use, the slide was examined under dark field illumination to observe the presence of dust particles in scratches on the surface of the glass. Most of these dust particles could be removed by wiping the slide with the standard cleaning tissues used for lenses. Drops of the liquid were taken from newly opened bottles by means of a pipette that had been cleaned in a glass-cleaning solution (sodium dichromate solution), distilled water, and acetone. With the exception of kerosene and olive oil, the remainder of the liquids studied were grade 2 (C.P. or better).

The photographs, see Figs. 2 and 3, are self explanatory and labeled as to the type of liquid, exposure time, and density distribution of the colloidal particles. The large streaks in several of the pictures are due to the movements of particles or clusters of particles during the exposure time. Other light corona are present in all of the pictures as a result of light reflections from surfaces that are not in focus. The density distribution of the colloidal particles may be estimated on the basis of the scale given at the top of Fig. 2. Inasmuch as the photographic plate cannot



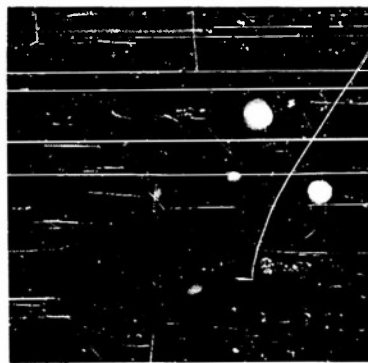
SCALE: UNITS OF 0.01 mm.



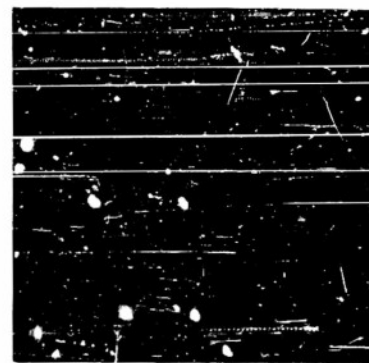
ACETONE  
45 SEC. EXP.  
LOW DENSITY



BENZENE  
35 SEC. EXP.  
MEDIUM DENSITY

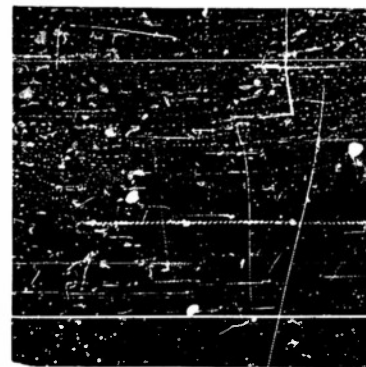


CARBON TETRACHLORIDE  
55 SEC. EXP.  
MEDIUM TO HIGH DENSITY



DISTILLED WATER  
45 SEC. EXP.  
VERY HIGH DENSITY

FIG. 2. PARTICULATE MATTER IN LIQUIDS



KEROSENE  
35 SEC. EXP.  
MEDIUM DENSITY



METHYL PHTHALATE  
45 SEC. EXP.  
VERY HIGH DENSITY



SPERM OIL  
45 SEC. EXP.  
MEDIUM DENSITY



OLIVE OIL  
45 SEC. EXP.  
LOW DENSITY



CASTOR OIL  
40 SEC. EXP.  
LOW DENSITY

FIG. 3. PARTICULATE MATTER IN LIQUIDS

approach the sensitivity of the eye in the ultramicroscopic observation of these particles, a qualitative description of the density distribution has been added. In the case of castor oil, the focal point is at the surface of the glass depression. The manner in which the dust particles have aligned themselves in the scratches on the surface of glass and the presence of occasional aggregates of particles can be readily seen in the photograph. In the case of volatile liquids such as acetone and carbon tetrachloride, the observation of colloidal matter proved very difficult. As a result of Brownian forces and the evaporation of the liquid, the particles were in continual motion. After the volatile liquid had completely evaporated, there remained a large number of particles on the surface of the glass. As shown by the photographs, the maximum density of particulate matter can be found in distilled water and methyl phthalate. Apparently these liquids have a greater affinity for dust particles.

The principal advantage of dark field illumination is that it allows one to observe objects that have too little contrast with their background or are too small for direct optical magnification whose limit is approximately 0.5 microns. Dark field techniques, unfortunately, do not allow one to observe the object itself but only the light reflected and refracted by the object. It is therefore difficult to gauge the actual size of the object (especially where the size of the object is comparable with the wavelength of light), although its presence and density distribution can be observed. Attempts to observe the colloidal matter in liquids by using an oil immersion 90x objective and 25x eyepiece were unsuccessful. The above observations, however, show conclusively that unless extreme precautions are taken, the presence of colloidal matter in liquids cannot be neglected in considering the tensile strength of the liquid.

#### E. Surface tension and other properties.

The only physical factor to have a significant effect on the surface tension of pure liquids is the temperature. If a liquid is in equilibrium with its vapor the surface tension of the liquid must obviously disappear at the critical temperature. To a first approximation one can write,

$$\sigma = K(T_c - T - T_x)$$

where

$K$  = constant of proportionality (characteristic for each liquid).

$T_x$  = correction ( $\sim 6^{\circ}$ ) for decrease of surface tension near  $T_c$

$T_c$  = critical temperature.

Other equations giving better approximations to experimental data have been developed by van der Waal, Eotvos, and others (see Bikerman [23] p. 48). The principal point in all of these equations is that the surface tension, and therefore the corresponding capillary pressure, will decrease almost linearly with an increase in temperature. For the case of bubbles in liquids the thermal conductivity of liquids is so much greater than that of gases, that the temperature of the liquid can be assumed to be independent of temperature variations within the gas. Thus the surface temperature will be assumed only to be a function of the liquid's temperature.

Other factors affecting the surface tension of a liquid are the presence of impurities or solutes. These variations of surface tension are not yet well understood and for the case of bubbles in pure liquids, need not be considered.

Up to this point of the discussion the principal parameter characterizing the surface layer of liquids or the interface between liquids and vapors, etc., has been the surface tension or free surface energy. The contact angle appearing in liquid-gas-solid interfaces can be considered to be a secondary parameter. In addition to its free surface energy, an interface may exhibit certain other dynamic properties. Pekeris [33] has presented evidence as to the existence of both a surface viscosity and specific surface resistance to diffusion. The surface viscosity has been shown by Rayleigh [34] to be due to the presence of contaminating particles which are ever present unless cautions are adopted to maintain extreme purity. On the basis of data regarding the velocity of rise of air bubbles in water, Pekeris proposed that up to radii of approximately  $4 \times 10^{-2}$  cm the effect of this superficial surface viscosity is to make the surface of the bubble dynamically rigid. Likewise, Pekeris has postulated the existence of a thin shell of fluid of thickness  $\delta$  and coefficient of diffusion  $D' < D$ , such that  $\beta = \lim_{\delta \rightarrow 0} \frac{\delta D}{D'}$  is finite. Inasmuch as the surface

viscosity is effective in a layer of molecular dimensions and is an undetermined function of the degree of contamination it will be neglected in later theoretical discussions. Similarly, the specific resistance to diffusion is effective in a layer of molecular dimensions and represents a higher order correction to the diffusion constant. Its effect will not be considered in the theoretical discussion regarding the growth of bubbles as a result of gaseous diffusion.

## III.

## THE EXPERIMENTAL APPARATUS

A. The mechanical apparatus.

As stated in the Introduction, the basic desire in this experiment is to measure the threshold for gaseous-type cavitation in liquids of different viscosities. This goal can be achieved only if one is able to control effectively the many variables encountered. Conditions are, therefore, desired so that cavitation may be produced within a system of such size and shape that wall effects will be avoided; that the liquid under test may be easily changed; and that little attenuation of the input sound signal will occur. In addition the following parameters require control: the gas content of the liquid; the purity of the liquid; the temperature of the liquid; the hydrostatic pressure upon the liquid; and the electrical characteristics of the system such as signal duration and frequency. Several of these variables had previously been taken into consideration by Blake ([3] p. 86) in the construction of an ultrasonic focusing tank and water degassing tower in this laboratory. This tank proved very successful for measurements in the steady-state (at one frequency) of the vaporous cavitation threshold of "moderately pure" water as a function of temperature and hydrostatic pressure. A decision was made to use this equipment and construct any modifications or additions that are necessary for the control of the supplementary parameters required in the study of gaseous cavitation. A brief account of Blake's apparatus is pertinent at this point. Changes made in the equipment will be described at appropriate places, and a description of the added superstructure will follow.

Blake's principal goal was to obtain a standing-wave system of sound waves focused by means of parabolic and plane reflectors. His mechanical apparatus consists of a cylindrical steel tank two feet in diameter and one foot high. Five inch hand holes in the bottom and top plates of the tank are provided for illumination of the interior, cleaning the tank, insertion of flasks, and insertion of probe hydrophones. A small side window is provided for visual observations into the central portion of the tank. The tank is connected by means of brass plumbing to a water pumping and degassing system. A large reservoir of water (approximately 30 gallons of distilled water are normally used) is circulated by a variable speed gear pump. Bourdon gauges allow for the continual measurement of pressure within the tank. The circulating water is degassed by spraying it through large pyrex "degassing" cylinders evacuated to the vapor pressure of water. These degassing cylinders are continuously evacuated by means of a direct connection to a heavy duty aspirator pump. The hydrostatic pressure within the tank is controlled through the proper use of cone valves within a range varying from vapor pressure up to 30 psi absolute. As noted by Blake, one difficulty with this apparatus was the pollution of the water, especially due to chemical reactions at surfaces of metals. He, therefore, had the tank lined with zinc. In spite of this precaution the water in the tank would remain clear for only a few days. Zinc carbonate developed at the surface of the metal and formed a suspension in the water. A slow electrolytic process continually took place resulting in gas generation and rust formation. In this present experiment on gaseous-type cavitation, the tank was carefully dismantled, and all rust sources (steel washers, screws, etc.) were removed. During the past year and a half only distilled water has been placed within the system, and the tank has been periodically scrubbed and cleaned. At present, distilled water left in the tank for as long as two weeks shows little contamination.

For control of the temperature, the tank is fitted with a copper heat exchanger coil through which water is pumped from a cylindrical reservoir heated by a four kilowatt electric immersion heater. Two thermostats, one located within the tank and the other within the reservoir are used to control the temperature of the water. Circulation of the

distilled water prevents the creation of temperature gradients, and the temperature can be controlled to within  $\pm 1/4^{\circ}\text{C}$ .

Inside the tank special reflectors are located so that the applied sound signal may be focused and concentrated within a small region. Three ultrasonic projectors are mounted in the upper plate of the tank. From this same plate, a parabolic mirror (spun from 1/16" sheet aluminum) and a flat mirror of 1/4" aluminum plate are suspended. The paraboloid's dimensions are: focal length, 3.5 inches; diameter, 22 inches; depth, 8 inches. Both mirrors had been previously covered with pressure-release Cell-tite Neoprene of 1/16" thickness. In this experiment, the older sheets of Cell-tite Neoprene were found to have undergone considerable surface hardening and aging. They were completely removed and replaced with a newer form of Cell-tite Neoprene which is considerably more pliable and appears to be less affected by contact with liquids over long time durations. As is shown in Fig. 4, sound waves are reflected and focused by the paraboloidal mirror. They then diverge, are reflected once more, and upon re-reflection from the upper mirror return along the same path. The standing wave system that is established has the advantage that it requires less power input for a given pressure amplitude and allows one to use a smaller physical system (with rapid build-up time) than would be required if plane waves had been used. The apparatus is a low Q system so that pulses may be efficiently transmitted. In addition, a standing-wave system has the added feature that the second order effect of "streaming" of the liquid at the focus is cancelled out. Adjustment of the paraboloid and flat mirrors leads to the proper impedance match to the projectors and the location of a pressure antinode at the focus.

For the study of gaseous-type cavitation certain additional requirements must be imposed upon any such mechanical system. Obviously it is extremely difficult to control the purity of 30 gallons of liquid. Colloidal impurities are ever present in spite of the care usually taken to use clean distilled water. In addition, the difficulty that would be encountered in pumping 30 gallons of a highly viscous liquid is apparent. Thus, for the maintenance of the purity of a sample as well as the practical use of small quantities, the decision was made to construct a special

flask system to hold the liquid to be examined in this study of gaseous cavitation. Such a system has to satisfy certain criteria. Acoustical power is an expensive and occasionally elusive quantity, and the flask has to be constructed such that a minimum amount of signal attenuation and distortion will ensue. The flask system must allow for the control of the amount of saturation of the gases within the liquid and be easily removed and positioned to provide for the examination of several different liquids. The temperature of the liquid and hydrostatic pressure upon the liquid must be subject to control. Finally, the entire apparatus must be easily cleaned so that the purity of the sample can be maintained. In practice it is not too difficult to meet these specifications and a special flask support and agitating equipment were added as a superstructure to Blake's apparatus. As shown in Fig. 5, this superstructure consists of a brass tube 1/2 inch in diameter and 17 inches in length, which is mounted in oilite bearings. A stuffing box at the top of the tube is provided for vacuum tight insertion of a probe hydrophone. Connecting tubes extend to the vacuum-pressure apparatus. The entire superstructure is superposed on a circular brass plate 5 inches in diameter, which fits in the upper-hand hole of the ultrasonic focusing tank. At the bottom of the brass tube is a flange support upon which flasks can be easily mounted and sealed. In order to saturate the liquid with gas it is agitated by driving the supporting tube in simple harmonic motion by means of an eccentric drive coupled through 5.3:1 reduction gears to a 3350 r.p.m., 1/40 horsepower motor. The motor operates on 115 d.c. and drives the entire mechanism at a speed of 632 revolutions per minute with a stroke of one inch. Stroboscopic examination of the vibrating system indicates very smooth operation at this speed and considerable agitation of liquids in the attached flask. This agitation process will be discussed in a later section and is necessary to prevent supersaturation or undersaturation of gas in the liquid under test.

The choice of flasks presents some difficulty. The flask must be sufficiently strong to withstand the vibrations, be easily cleaned, result in little loss or distortion of the applied ultrasonic signal, and be several wavelengths in diameter so that surface effects can be avoided. Several types of flasks were first tried. A cylindrically shaped flask was made

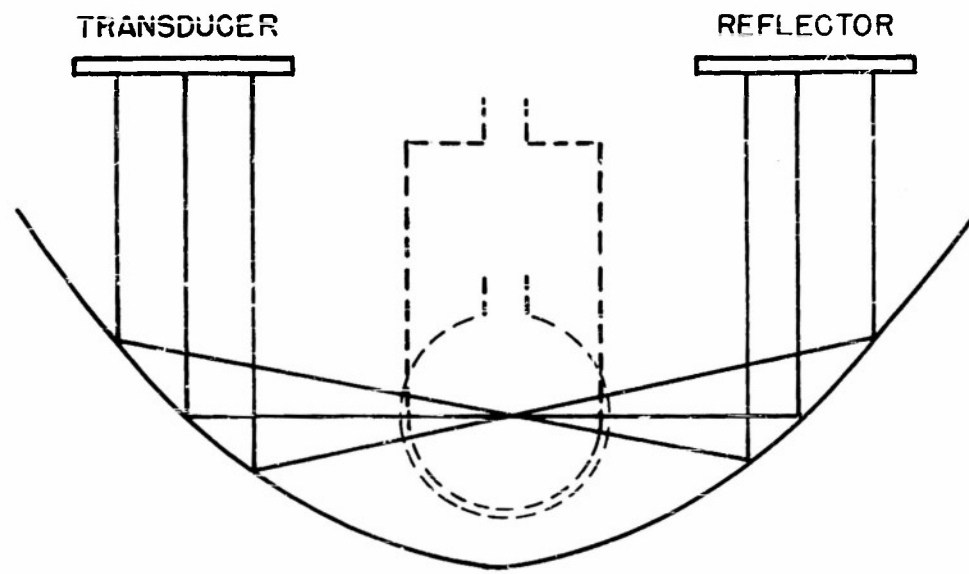


**FIG. 4. PARABOLIC REFLECTING SYSTEM**

SCALE - 1:4

FOCAL LENGTH - 3.5"

CYLINDRICAL AND SPHERICAL FLASKS  
SHOWN IN PLACE

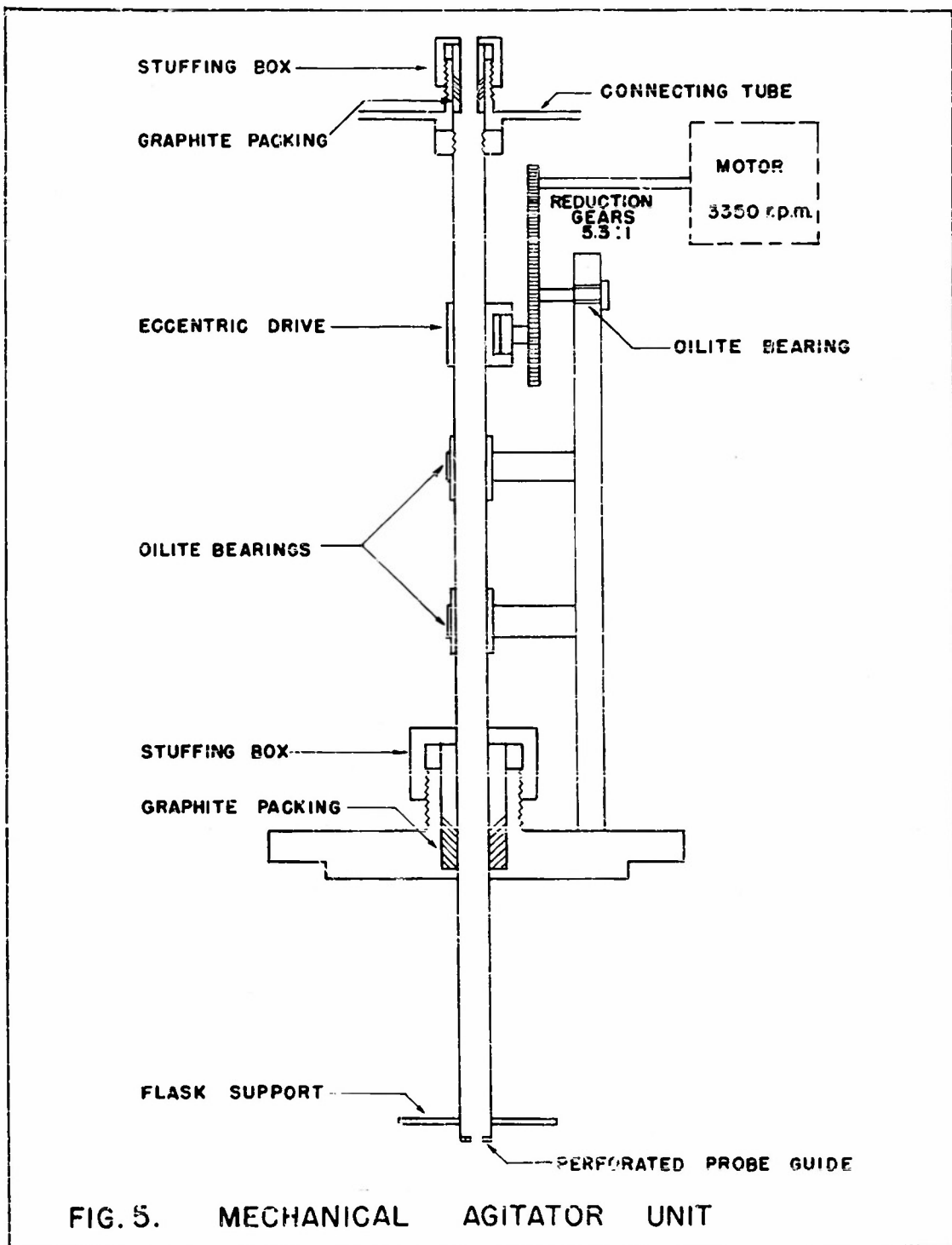


FIG. 5. MECHANICAL AGITATOR UNIT

out of standard-walled glass tubing four inches in diameter. Both signal attenuation and distortion occurred as a result of the wall thickness and shape of the flask. Similarly, ordinary spherical pyrex flasks have a wall thickness of approximately  $1/16"$ , and this thickness resulted in an attenuation of approximately 1 db. This loss is readily apparent on the basis of the analysis of the transmission of sound at normal incidence through three media. Several textbooks [ 35 ], [ 36 ] discuss this academic problem. The sound transmission coefficient,  $a_t$ , is defined as the ratio of the transmitted sound intensity in the third region to the incident sound intensity in the first region. The intermediate medium is referred to as region two. One can show that

$$a_t = \frac{4d_{13}}{(d_{13}+l)^2 \cos^2 k_2 l' + (d_{12}+d_{23})^2 \sin^2 k_2 l'} ,$$

where

$$d_{12} = \frac{\rho_2 c_2}{\rho_1 c_1}$$

$$d_{23} = \frac{\rho_3 c_3}{\rho_2 c_2}$$

$$d_{13} = \frac{\rho_3 c_3}{\rho_1 c_1} = d_{12} d_{23}$$

$$k_2 = \frac{\omega}{c_2}$$

$l'$  = thickness of region 2.

If  $k_2 l' \ll 1$ ,

$$a_t \approx \frac{4d_{13}}{(d_{13}+l)^2} ,$$

and the effect of region 2 can be neglected, that is, the walls of the flask can be disregarded if  $k_2 l' \ll 1$ . For pyrex glass at a sound frequency of 60 kc/s,  $k_2 = 0.628$ , and it is necessary that

$$l' \ll 1.59 \text{ cm} = l''$$

For the present experiment it was decided to choose  $l'$  between  $(1/50)l''$  and  $(1/20)l''$  ( $l'' = 0.032$  to  $0.08$  cm), such that the presence of the pyrex walls would cause a small loss, between 0.06 to 0.28 db. Two types of flasks, one spherical and the other cylindrical were constructed. To

make the spherical containers, 48 mm glass tubing was specially blown into spheres with an average diameter of 4 1/2 inches and uniform wall thickness of  $0.014 \pm 0.002$  inches. Examination of these containers under a polariscope indicated no strains except at the turn of the 2" neck of the flask. For the purposes of mounting, each flask is carefully fitted with a brass cap. This cap is cemented to the 2" neck with Cenco Sealstix, a new form of De Khotinsky cement. The container is then tightly secured to the flask support by means of three screws and an insert washer. Finally, after cleaning and filling with the liquid to be studied, the flask is positioned centrally around the focus of the paraboloid in the tank so that measurements can be made.

The cylindrical containers were obtained by drawing and rounding off a piece of 4 inch I.D. pyrex glass tubing. The wall thickness of the lower 3 1/2 inches of the container was  $0.033 \pm 0.010$  inches. This flask is fitted with a 4 inch brass cap, secured to the flask support, and positioned so that measurements can be made.

Figure 6 shows the air-vacuum system used to control the hydrostatic pressure upon the liquid in the flask container. Compressed air obtained from an air line is passed through drierite and a dry ice-acetone trap. The hydrostatic pressure over the liquid in the flask can be raised as high as 1500 mm of Hg. The vacuum pump is similarly used to reduce the pressure to approximately 5 mm of Hg. A large pressure range is available, and agitation of the liquid permits one to maintain gas saturation in the liquid at all times. The equipment is also adaptable for use with other gases besides air.

#### B. The diffraction of sound by the paraboloidal mirror.

The diffraction of sound or light by a concave spherical reflector has been treated by several authors, for example, Born [37], Preston [38], and Griffing and Fox [39]. In all of these cases first order diffraction theory has been used in that each element of the reflector has been considered to be a point source upon which the influence of neighboring elements is negligible. This requirement can be satisfied if the wavelength of the diffracted wave is sufficiently short such that the contributions of neighboring elements to the selected element are random in

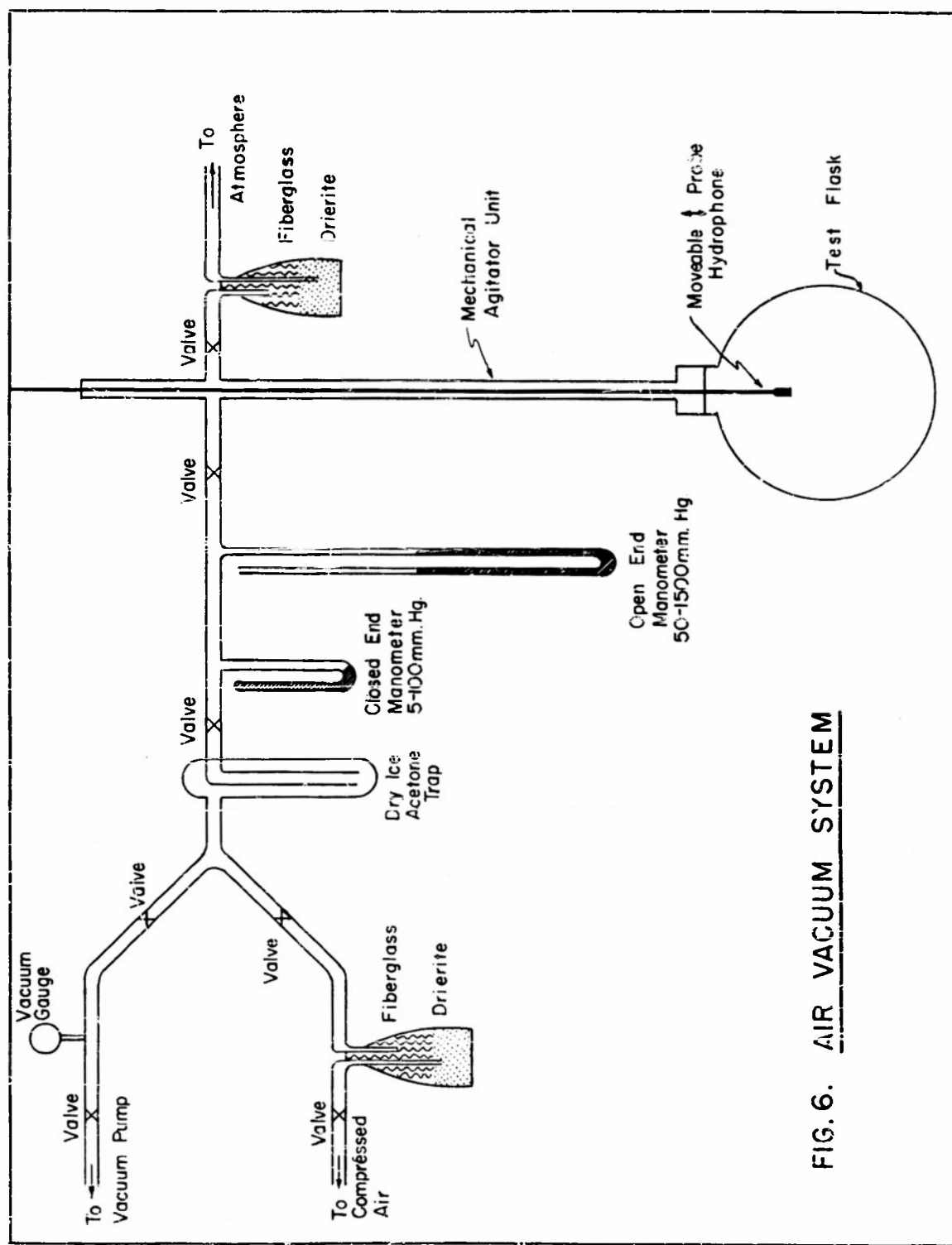


FIG. 6. AIR VACUUM SYSTEM

phase and effectively cancel themselves out through interference. This condition is usually stated in the form that the reflector must subtend many wavelengths.

The problem of diffraction by a paraboloidal reflector is highly complicated. On the basis of first order diffraction theory, Rocard [40] has derived a formula that describes the pressure wave diffracted by a concave parabolic reflector (See Fig. 7 on the following page).

$$\begin{aligned}
 \frac{P_2}{P_1} = & i \frac{4\pi f}{\lambda} e^{-i \frac{4\pi f}{\lambda}} \left\{ \ln(1+u) - \frac{X}{f} \frac{u}{(1+u)^2} \right. \\
 & + \frac{X^2}{4f^2} \left[ \frac{14u + 15u^2 + 20u^3 + 5u^4}{6(1+u)^4} - \frac{8\pi^2 f^2}{\lambda^2} \left\{ \ln(1+u) - \frac{2u^2}{(1+u)^2} \right\} \right] \\
 & + \frac{Y^2 + Z^2}{4f^2} \left[ \frac{12u + 36u^2 + 28u^3 + 7u^4}{6(1+u)^4} - \frac{8\pi^2 f^2}{\lambda^2} \frac{u^2}{(1+u)^2} \right] + \dots \\
 & + i \frac{\pi f}{\lambda} \left[ \frac{X^2(15u + 12u^2 - 8u^3) + (Y^2 + Z^2)(9u^2 - 13u^3)}{6(1+u)^3} \right] \\
 & \left. - 2fX \left[ \ln(1+u) - \frac{2u^2}{(1+u)^2} \right] + \dots \right\},
 \end{aligned}$$

where

$P_2$  = pressure of the diffracted sound wave

$P_1$  = pressure of the incident plane longitudinal wave

$X, Y, Z$  = coordinates with reference to the focal point of the paraboloid

$f$  = focal length of the paraboloid

$u = h/f$

$h$  = height of the paraboloid

The series for  $P_2/P_1$  has been obtained by assuming that the incident plane wave completely fills the paraboloid. This series is only useful if  $\lambda < 2f$  and the distance of the point  $(X, Y, Z)$  from the focus is less than a

wavelength. One can readily see that the amplitude of the pressure ratio at the focus ( $X=0, Y=0, Z=0$ ) is simply

$$\left| \frac{P_2}{P_1} \right| = \frac{4\pi f}{\lambda} \ln \left( 1 + \frac{h}{f} \right).$$

The apparatus used in this experiment for the reflection and focusing of the acoustical signal is somewhat similar to a shorted electrical transmission line driven by a generator whose internal impedance matches that of the line. One round trip of the signal is nearly sufficient to establish steady-state conditions. Hence the system can be looked upon as one in which two waves of equal amplitudes are traveling in opposite directions. This fact has been borne out by observations of the build-up and decay of the sound pressure at the focus of the paraboloid. The steady-state pressure is reached (within a few per cent) in exactly two steps. The first step is due to the direct wave while the second step is due to the reflected wave. Thus, if  $S$  is the effective radiating area - the face of one transducer, the total area of the incident plane wave in this apparatus is approximately  $6S$ . Let  $P$  represent the input power to a transducer whose efficiency is  $\eta$ . Then

$$P_1 = \left( \frac{2pc\eta P}{S} \right)^{\frac{1}{2}}$$

and

$$\left| \frac{P_2}{P_1} \right|_{\text{focus}} \approx \left( \frac{2pc\eta P}{S} \right)^{\frac{1}{2}} \left[ \frac{4\pi f}{\lambda} \ln \left( 1 + \frac{h}{f} \right) \right] \frac{6S}{S'}$$

where

$S'$  = area of the aperture of the paraboloid.

For the system used in this experiment the three transducers are driven in series. The effective radius of each transducer is approximately  $1.6\lambda$ . The focal length of the paraboloid is  $3.5\lambda$ ; the height is  $8\lambda$ ; the diameter of the aperture is  $22\lambda$ ; and  $\lambda$  is one inch. For an input

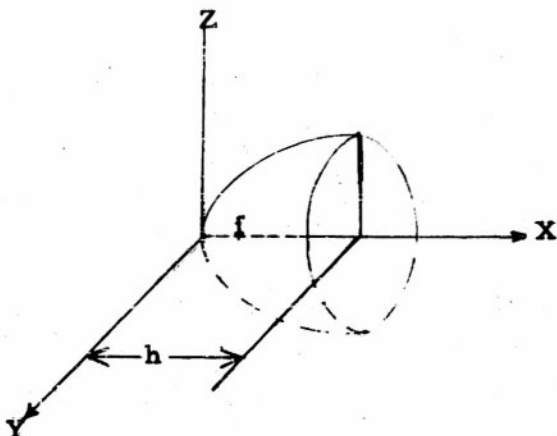


Fig. 7.

power of 120 watts to the three transducers and an efficiency of 30% for each transducer,

$$\left| \frac{P_2}{P_1} \right|_{\text{focus}} \approx 5.5 \text{ atmospheres.}$$

Experimentally the maximum pressure measured at the focus is 5.4 + 1 atmospheres.

Similar theoretical results can be obtained if one assumes that the portion of the surface of the paraboloid upon which the plane wave is incident (see Fig. 4) can be approximated by a concave spherical reflecting surface. This approximation can be made if the latus rectum of the paraboloid is much greater than a wavelength. The focal length  $f'$  of the concave spherical reflector will be one half the latus rectum of the paraboloid or  $7\lambda$ . One can readily show (see Griffing and Fox [39]) that the pressure ratio is

$$\left| \frac{P_2}{P_1} \right| = \frac{6S}{f'\lambda} \frac{2J_1(Z)}{Z},$$

where

$$Z = \frac{2\sqrt{\pi S}}{f'\lambda} (r_f)$$

$r_f$  = radial distance in the focal plane

Then,

$$\left| \frac{P_2}{P_1} \right|_{\text{focus}} = 6 \left( \frac{2\pi S}{f'\lambda} \right)^{\frac{1}{2}} \frac{S}{f'\lambda}.$$

Using the same values as those used above

$$\left| \frac{P_2}{P_1} \right|_{\text{focus}} \approx 5.7 \text{ atmospheres.}$$

Theoretically the first pressure minimum in the focal plane should occur at a radial distance from the focus given by

$$[r_f]_m = 0.61 f' \lambda \sqrt{\frac{\pi}{S}} \approx 6.8 \text{ cm}$$

Experimental observations on the diffraction pattern show that the first pressure minimum occurs at a vertical distance of approximately 6.1 cm.

In the foregoing discussion various aberrations, undesired reflections, and losses due to scattering and dissipation have been neglected. In addition the sound wave incident upon the reflector has been assumed to be a

plane wave. This wave will have its own diffraction pattern, but when the source of sound is large compared to the wavelength and at the correct distance from the reflector, the waves falling upon the reflector can be best described as plane waves. These requirements had been taken into account in the construction of the paraboloidal reflecting system (see Blake [3], p. 87). In general, first order diffraction theory effectively shows how the acoustical signal is focused.

### C. The electronic apparatus.

The electronic apparatus used in the experiment can be divided into a transmitting and a receiving system. In brief, the transmitting system consists of three magnetostrictive transducers driven by an oscillator and appropriate power amplifiers with provision for pulse modulation. The receiving system is simply a calibrated hydrophone whose response is represented on either a voltmeter or cathode ray oscilloscope. The principal design of the entire electronic equipment is to provide for the generation of high intensity electrical signals at 60 kc/s which are converted into acoustical waves whose absolute pressure can be measured.

The transducers used are three General Electric Co. type MS-4 magnetostrictive units obtained through the courtesy of the Office of Naval Research. These transducers replaced the previous ones used by Blake and exhibited higher efficiency and less electrical break-down difficulties. Their circle diagrams obtained by impedance bridge measurements are shown in Fig. 8. As shown by the diagram, the units are well matched and have an operating frequency of approximately 60 kc/s. Each unit is made up of a 3 by 6 inch rectangular array (split into halves) of 28 individual magnetostrictive driving elements. These elements are narrow band resonant devices. The two halves of each transducer are wired in series through a series resonating 0.01 microfarad capacitor, and all transducers are driven in series with the same driving current. Each half presents a resonant impedance in air of approximately  $130 + j 123$  ohms. Thus the total input impedance at resonance is approximately 780 ohms under air loading. The input signal is obtained from a Western Electric type 17B beat-frequency oscillator. Its output is coupled to a pulser amplifier. The system consists of a pulser unit designed by A. Janszen of this laboratory; a driver amplifier designed by G. Blake; and

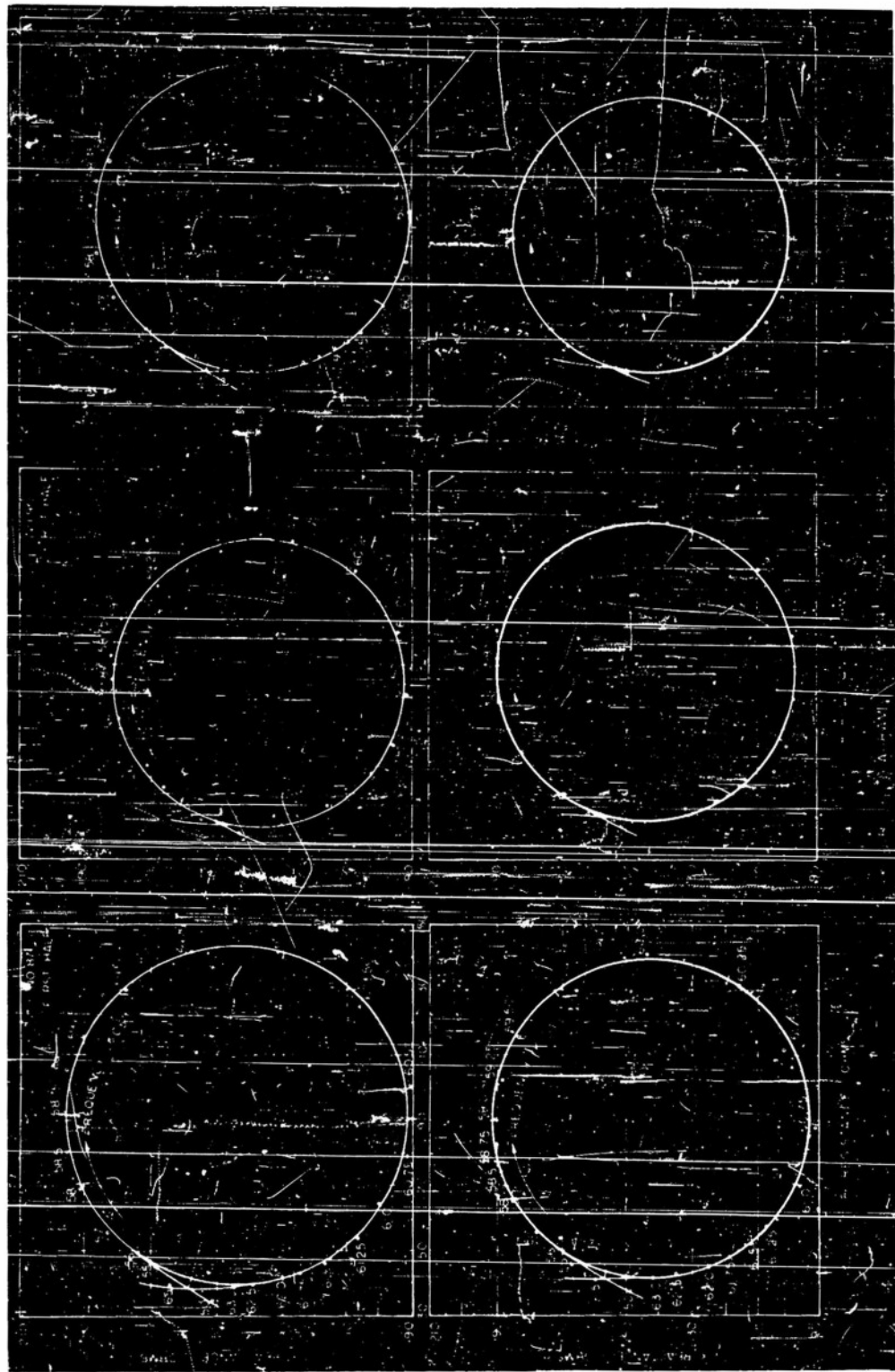


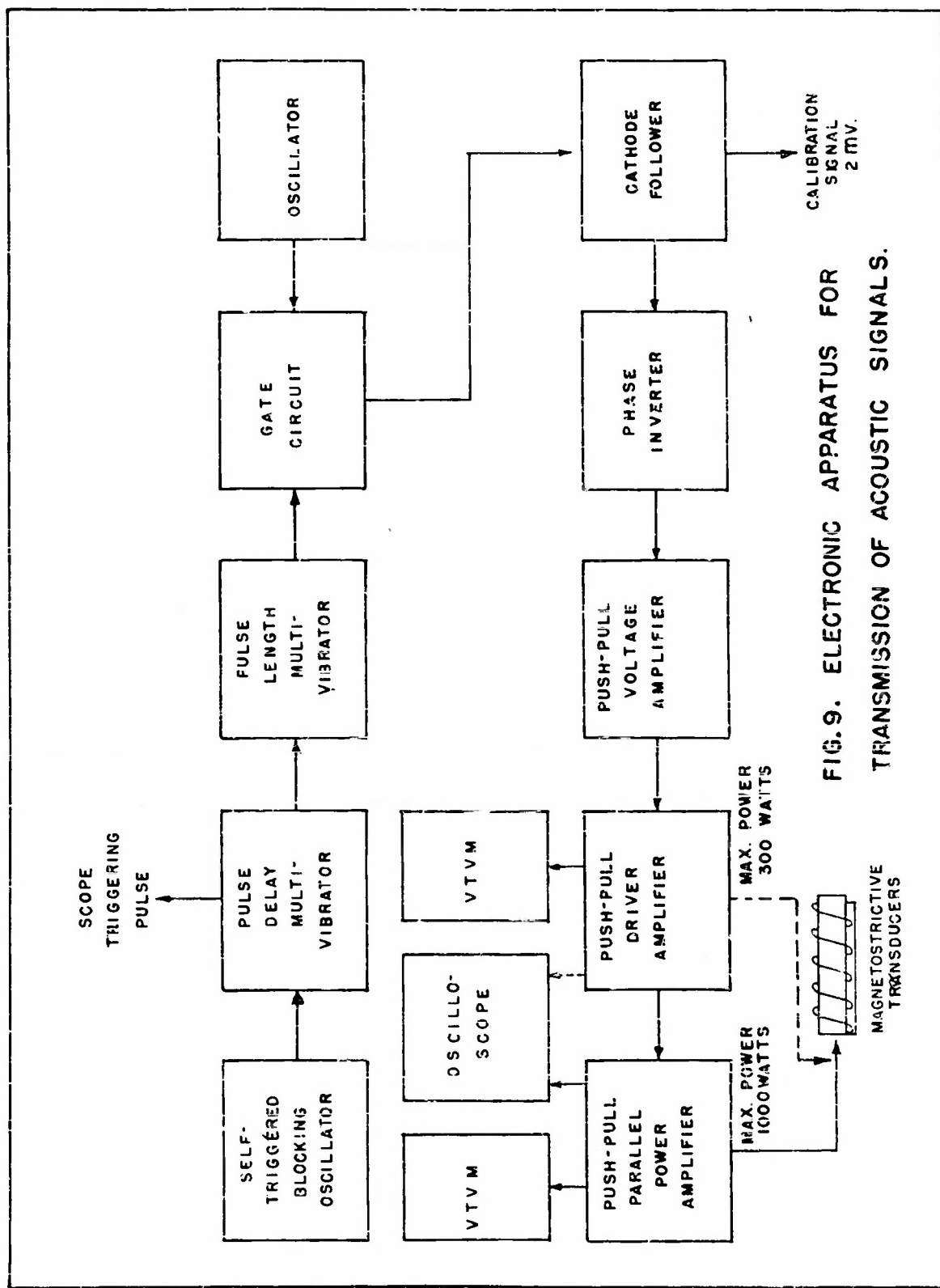
FIGURE 8

a power amplifier rehabilitated for this experiment. A block diagram of the electrical transmitting apparatus is shown in Fig. 9. The pulser is made up of a blocking oscillator whose pulse repetition rate can be set at any one of the following values: 0.3, 1, 3, 10, 30, or 100 pulses per second. A delay multivibrator is provided to allow for signal delays (in addition to a triggering pulse for the oscilloscope) of 1, 3.3, 10, 33 and 100 milliseconds. The pulse length is controlled by means of a multivibrator to be: 0.3, 1, 3.3, 10, 33, 100, 333 milliseconds. This pulse is used to gate the input oscillator signal which is then passed through a voltage amplifier into a driver amplifier. The driver amplifier uses two type 828 power pentodes in a push-pull arrangement. Fixed bias, screen, and plate supplies are provided for the equipment. Provision is also made for the steady-state use of the apparatus and for the removal of a 2 millivolt signal that is used to calibrate the output circuit of the receiving apparatus. This amplifier supplies a maximum power of 300 watts into a matched 500 ohm load.

The output of the driver amplifier is coupled through an output transformer either to the MS-4 transducers or to a 1000 watt power amplifier unit. In studies on pure and highly viscous liquids high-power generation is required. The power amplifier is a Western Electric type 100A amplifier that has been extensively modified for this experiment. The unit uses four type 308B power tubes operated class B1 in a push-pull-parallel arrangement. This unit had been designed originally for use at 1 kc/s and was in rather poor condition. Considerable labor was required to rehabilitate the unit, and in the final analysis it might have been easier to construct a new unit. Breakdowns, however, are unpredictable, and replacements were made as they were needed. The equipment has been installed with new input and output transformers obtained from the Audio Development Company. These transformers operate in the frequency range between 20 and 100 kc/s. A 500 ohm, 1000 watt, non-inductive dummy load has been placed in the output circuit so that it can be used for test purposes. Matched 1 ohm resistors have been wired across the central leads of the output transformer and center-tapped to ground. A voltmeter and oscilloscope across one of the resistors are used to monitor the output signal. For safety measures a 1/32 inch spark gap has been

placed across the output leads, and a shorting bar has been installed so that the positive side of the plate supply filter condenser can be grounded when the equipment is not being used. The plate voltage supply was made up of three type 249C gaseous rectifier tubes used with a three phase 220 volt input. These tubes have been replaced by type RCA 866A gaseous rectifier tubes. The grid bias supply is controlled by means of a variac in the input circuit. In normal operation the grid voltage is set for minimum signal distortion at maximum operating power. The plate voltage is controlled by a remote switch, and the tubes are cooled by means of a large circulating fan. During the course of operation several switches and resistors have been replaced. A new filament transformer has been installed, and grid retardation coils have been replaced with 10 ohm resistors. The unit now functions efficiently and provides an output of 1000 watts at 60 kc/s.

The receiving, or ultrasonic detection unit, is similar to that used by Blake. The probe hydrophones constructed for this experiment are made of small cylinders of hand-drawn nickel tubing. The cylinders are 1/8 inch long with an inside diameter of 1/8 inch and a wall thickness of 0.0065 inches. The inside of the cylinder is lined with a single-layer scroll of bond paper and a piece of cell-tite neoprene approximately 0.018 inches thick. This thin sheet of neoprene was obtained by slicing a 1/16 inch piece of cell-tite neoprene along its thickness dimension. The thin sheet obtained in this manner was examined microscopically to see that it still contained a complete layer of isolated air cells. These cells serve as an internal pressure release backing. The nickel cylinder is then dipped in red glyptal and baked. A toroidal coil of approximately 45 turns of red enameled number 36 wire is next wound on the tubing. The unit is mounted on either a 1/8 inch bakelite or polystyrene rod which is supported by a brass tubing 1/8 inch or 1/4 inch in diameter. Electrical connections are made through the brass tubing. Finally the probe is dipped into a solution of Westinghouse Tuffernel (a sealing material that is resistant to acids, alkalis, and oils), and baked once again. A 40 ampere peak discharge of 2.5 milliseconds time constant is used to magnetize the nickel. Inasmuch as the work involved in making these magnetostrictive probes is very tedious a 1/8 inch I.D. tube of barium titanate has been obtained from the Brush Development Corporation for use in future experiments.



## TRANSMISSION OF ACOUSTIC SIGNALS.

The probe hydrophone has a low output impedance of approximately 1.2 / 55° ohms at 60 kc/s. In order to avoid coupling from the high power circuits, care has been taken to provide good shielding, grounds, and isolation. As shown in Fig. 10, the output of the hydrophone is fed directly to a line transformer consisting of a 36 turn primary on a toroidal dust-core choke, (used as a secondary) type W.E. D170711 of 366 turns and 24 mh. A type W.E. 179B shielded transformer matches the line to a high impedance Ballantine voltmeter input and Dumont type 208 oscilloscope modified for single sweep operation. Output voltage readings are directly transformed to pressure readings. The output circuit is calibrated by means of an insert voltage of 2 millivolts obtained from the cathode follower unit of the transmitting apparatus. The probes constructed for this experiment have been calibrated on the basis of comparison-measurements with a probe previously calibrated by Blake. Their sensitivities average approximately -146 db, the best probe having a sensitivity of -145 db. The probes that employ a layer of cell-tite neoprene as a pressure release backing have an average sensitivity approximately 1 db greater than the probes that depend for pressure release backing upon the air that is entrapped within the windings.

D. Preparation of flask and liquids to be tested.

The liquids tested in this experiment were generally classified as grade II, that is, C.P. In Chapter II it was shown that all of these liquids contain colloidal matter suspected of being dust particles approximately 0.5 microns in diameter. The complete removal of these colloidal particles is beyond the bounds of this experiment. Because of the effect of Brownian motion the particles will not settle out of solution but rather maintain a distribution similar to that of gases in the atmosphere. Even if Brownian forces were not present the settling process would depend upon the opposing Stoke's and gravitational forces. A simple calculation (see Dalla Valla [26], p. 31) can be based on an equation that equates the inertial force of the particle to the difference between the gravitational force and the opposing viscous or Stoke's force.

Thus

$$m \frac{dv}{dt} = mg \frac{\rho - \rho_0}{\rho} - 3\pi d v$$

where

$m$  = mass of the particle  
 $v$  = velocity of the particle  
 $t$  = time  
 $g$  = acceleration of gravity  
 $\rho$  = density of the particle  
 $\rho_o$  = density of the fluid medium  
 $d$  = diameter of the particle  
 $\mu$  = viscosity of the fluid medium.

The solution of this equation is

$$s = v_m t - (v_m - v_o) \frac{m}{3\mu\pi d} \left[ 1 - e^{-\frac{3\mu\pi d}{m} t} \right],$$

where

$s$  = distance traveled by the particle  
 $v_m = (\rho - \rho_o) \frac{gd}{18\mu}$  = maximum settling velocity of the particle  
 $v_o$  = initial velocity of the particle.

For the case of water in a flask 4 1/2 inches in diameter, the maximum settling time would be approximately 56 hours. In more viscous liquids the settling time would increase in almost direct proportion to the increasing viscosity. In view of these large settling times and especially the effect of Brownian forces, the settling process obviously provides only a partial solution to the problem of the removal of colloidal impurities.

Centrifuging methods offer the best way to remove particles of this size. However, elaborate apparatus is required, and such equipment was not readily available for this experiment. In addition, while Harvey [24] found very strong centrifuging (800 G) capable of removing "macro-nuclei," it was not sufficient for the removal of "micronuclei." Thus the presence of some form of nuclei in the liquids is accepted in this experiment as being an integral part of the liquid.

The pyrex flask used to hold the liquids presents its own difficulties with regard to cleanliness. A "dirty" point on the surface of the flask often serves as the nucleus for cavitation and presents a weak point in the system. When this event occurs, it is necessary to disregard the measurements and reclean the flask. Various methods have been adopted for

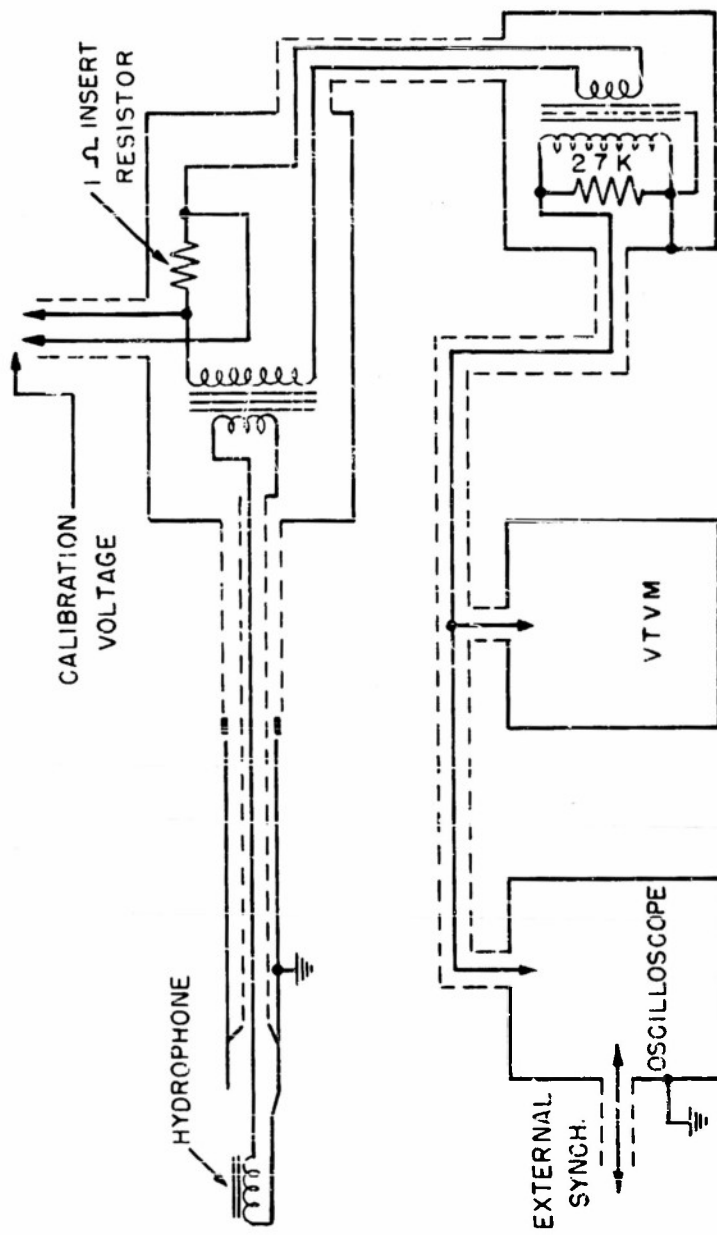


FIG. 10. ELECTRONIC APPARATUS FOR RECEPTION  
OF ACOUSTIC SIGNALS

cleaning the inside surface of the flask. The method finally adopted is as follows: The flask is first washed with the common laboratory cleaning solution made by mixing a solution of saturated sodium dichromate and concentrated sulphuric acid. This cleaning, which removes oil films is followed by a distilled water rinse. The flask is then washed with Alconox, a common laboratory detergent, and once more rinsed with distilled water. Finally, acetone is used to take up any water remaining in the container. After having been allowed to dry, a small amount of the liquid to be tested is used as a wash for the flask, and then the liquid is added. Several flasks are used throughout the experiment, and each is washed in the same manner. The outer surface of the glass is simply washed with distilled water and a small amount of aerosol so as to wet the surface for better contact with the external flowing water.

One may also view the presence of absorbed and entrained gas in the fluid as another form of colloidal or extraneous matter. In this experiment, however, the saturation of air in the test liquids is highly desired, and the apparatus is constructed so as to allow for the maintenance of saturated conditions. It is, therefore, pertinent to consider at this point the manner in which the supersaturation, saturation, or undersaturation of gases occurs in liquids.

#### E. The saturation of gases in liquids.

The standard treatment of the solution of gases in liquids is based on Henry's well-known law. This law states that at equilibrium, if a gas does not react chemically with the liquid solvent, the free volume of dissolved gas in the liquid is directly proportional to the absolute pressure of the gas. In mathematical form,

$$V_e = S \frac{P_e}{P_o} V_t$$

where

$V_e$  = equilibrium volume of free gas dissolved in liquid

$V_t$  = equilibrium volume of liquid

$P_e$  = equilibrium gas pressure above liquid

$P_o$  = atmospheric pressure

$S$  = solubility constant in per cent.

For any gas concentration dissolved in the liquid there is at constant temperature an equilibrium pressure,  $p_e$ . Suppose  $p_g$  represents the actual gas pressure over the surface of the liquid. Then, if  $p_e = p_g$ , equilibrium exists; if  $p_e > p_g$ , the liquid is supersaturated with gas, and evolution can take place; if  $p_e < p_g$ , the liquid is undersaturated with gas, and absorption can take place. The verb "can" is used with care. The existence of a supersaturated condition does not necessarily mean that the evolution of gas will occur. The ability of liquids to remain in a highly supersaturated state has long been investigated. In 1866, Gernez [41] was the first to experiment with the supersaturation of gases in water. Later, Kenrick, Wismer, and Wyatt [42] were able to supersaturate water up to 100 atmospheres of excess pressure. Both carbon dioxide and oxygen yielded similar results. Metschl [43] made similar observations. He found that in most cases, with an excess supersaturation pressure of 4 atmospheres, violent mechanical agitation of the liquid was necessary to shake out the gases. In addition, his results indicate that the amount of agitation bears an inverse relation to the solubility of the gas in the liquid. More recent work in this field has been conducted by Schweitzer and Szebehely [44]. Their experiments were concerned primarily with rate of gas evolution (and absorption) in supersaturated (and undersaturated) liquids. The liquids that they tested were placed in a cylindrical container of 3400 cc and shaken with a frequency of 400 cycles per minute and with a stroke of one inch. No liquid subject to this mechanical agitation was able to maintain a supersaturated state. In order to measure the rate of gas evolution, the gas pressure over the liquid was reduced from the equilibrium pressure,  $p_e$ , to a new gas pressure,  $p_g$ . The closed system was then agitated, and the gas pressure over the liquid was measured as a function of time. Finally a new equilibrium pressure,  $p_e'$ , was reached where  $p_g < p_e' < p_e$ . The pressure  $p_e'$  can be represented by the equation,

$$p_e' = \frac{V_g p_g + V_l s p_e}{V_g + V_l s}$$

where

$V_g$  = volume of gas above the liquid.

Likewise,

$$V = S \frac{P_e'}{P_o} V_l - \frac{P - P_e'}{P_o} V_g ,$$

where

$V$  = volume of free gas dissolved in liquid at time  $t$   
 $P$  = gas pressure above liquid at time  $t$ .

Schweitzer and Szebehely assumed that the rate of evolution is proportional to the supersaturation (and the rate of solution to undersaturation) and obtained the relationship,

$$P_e' - P = \frac{SV_l}{V_g} (P_e - P_e') e^{-kt}$$

where

$$k = \frac{\ln 2}{T_E}$$

$T_E$  = time required to half-complete the gas evolution process.

This equation was well supported by extensive experimentation. The half life is a constant with respect to the apparatus used to obtain the experimental data.  $T_E$  obviously depends upon the method of agitation and the gas-liquid volume ratio for a given gas-liquid combination. The solution or absorption process is completely analogous to the evolution process, and the experiments of the above authors showed that the half life for solution is always greater than that for evolution. Schweitzer and Szebehely tested lubricating oils, fuels, and distilled water. With the exception of distilled water, the half life of evolution,  $T_E$ , increased with decreasing solubility, with increasing viscosity, and with increasing surface tension. Szebehely [45] obtained the relationship,

$$T_E = 0.263 v^{0.81} \text{ seconds (at } 70^{\circ}\text{F}) ,$$

where

$v$  = the kinematic viscosity in centistokes.

On the basis of these data, Schweitzer and Szebehely reach some interesting conclusions regarding cavitation and gas evolution. The authors suspect that the true tensile strength of liquids is extremely high, and that most measurements have resulted in relatively low values because of the difficulty in avoiding contamination and surface effects. In fact, most

measurements only yield values related to the weakest link of the chain which is often the adhesion between the liquid and some surface or between the liquid and some entrained gas in the form of microscopic or sub-microscopic bubbles. This idea of the weakest link in a liquid has long been recognized by research people in the field of cavitation and has been discussed in Chapter II of this memorandum. Schweitzer and Szebehely mention, however, that a quiescent liquid which has been in equilibrium with air for a sufficient length of time will contain a zero amount of entrained air dispersed in the liquid in the form of bubbles and a saturation amount of dissolved air. The entrained air in an agitated liquid will reach a maximum at a certain degree of agitation while maintaining a saturation amount of dissolved air. This observation, explains why flowing water will cavitate when subject to less negative pressure than that required to cavitate still water.

Somewhat similar hypotheses have been presented in Chapter II of this paper. It has been shown, however, that even a quiescent liquid will contain a finite amount of "entrained" air as a result of de novo formation and/or the stabilization of gas within crevices.

#### IV.

#### EXPERIMENTAL RESULTS

##### A. Description of gaseous-type cavitation.

The presence of gases in liquids has long been known to increase the susceptibility of liquids to cavitation. Many authors have even felt that a gas-saturated liquid would be unable to sustain at atmospheric pressure a peak negative pressure much greater than one atmosphere. This suspicion has been borne out by experiments on water saturated with air. Except for the experimental work of Briggs, Johnson, and Mason [9], little else has been done to measure the threshold for ultrasonic cavitation in liquids of varying physical properties. Thus, the observations of Briggs et al indicate the form in which cavitation will occur in various liquids. This observed cavitation has been described as vaporous-type cavitation by Briggs et al, while Blake [3] has noted that the cavitation so described is the same as the gaseous-type cavitation and distinct from the vaporous-

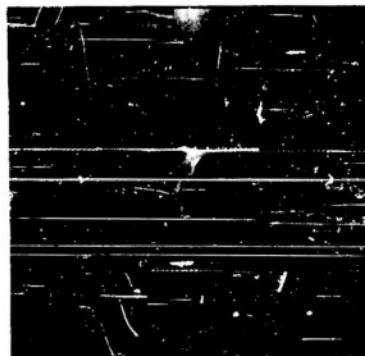
type cavitation that he observed in water. Not only is the theory of gaseous-type cavitation in an undeveloped state, but also the observations as to what is gaseous-type cavitation. It is therefore profitable to discuss qualitatively the forms of cavitation bubbles observed in liquids purposely saturated with air.

In order to make these observations, liquids were saturated with air in a closed system at a pressure of approximately 760 mm Hg. The mechanical agitator unit previously described in Chapter III was used to attain saturated conditions. With the probe in the center of the liquid and at the focal point of the ultrasonic signal, the liquid could be easily cavitated. Once a liquid had been cavitated it was essentially "poisoned," that is, further cavitation was readily obtainable with a lower sound pressure even though the probe was removed from the focus. Flash photographs were taken of the cavitating liquid. The duration of the flash is about 1/4 milliseconds, a rather long time exposure compared to a period of 1/60 millisecond. A 3 1/4 inch by 4 1/2 inch Linhof camera was used with a Carl Zeiss Tессar f 4.5 lens whose focal length is 15 cm. The principal advantage of this camera was its excellent lens and ground glass focusing back so that pictures could be prefocused. Kodak super panchro-press, type B, cut film was used for all photographs.

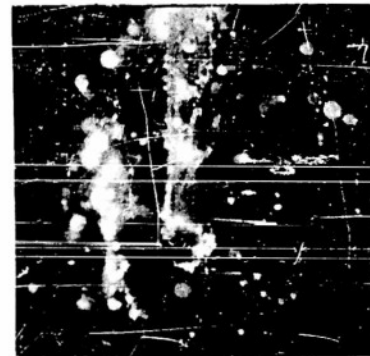
A selected group of pictures is shown in Figs. 11 and 12. Figure 11A shows a picture of the probe hydrophone in water. At a relatively low power input small streamers or clouds of bubbles issue from the focal region. These bubble streamers have a fog-like appearance. It is extremely difficult to estimate the sizes of these bubbles, but knowing that the diameter of the polystyrene probe support is 1/8 inch, it appears that the bubble diameters are less than 0.1 mm, the resonant diameter at 60 kc/s for bubbles in water. The rings in the upper part of the photograph are light diffraction rings. With an increase in the power output, the state shown by Fig. 11B results. In this photograph both vaporous and gaseous cavitation is taking place. The large bubbles showing excellent spherical symmetry are vaporous cavitation bubbles. Their maximum diameter is approximately 3 mm. The small bubbles usually found in streamers which move rapidly about the liquid are gaseous cavitation bubbles with diameters ranging from something under 0.1 mm to 0.5 mm. Because of the distortion

of the sound field by the presence of so many vibrating bubbles little can be observed as to the forces acting upon the individual bubbles. At lower power inputs, however, the bubbles tend to migrate to the pressure nodes of the standing wave sound field. A form of cavitation somewhat similar to that observed in water, can be observed in Fig. 11C, which shows a picture of cavitation in methyl phthalate. The cavitation first appears in the form of streamers of bubbles approximately 0.1 to 0.25 mm in diameter. These streamers issue upward in the liquid in either a vertical or spiraling manner. Occasionally simple bubbles will be trapped in a vortex and execute a circular motion or remain in the center of a vortex of very small fog-like bubbles. With an increase in power output the rate of formation of bubbles increases and rather large bubbles with a maximum diameter of approximately 1 mm appear in the liquids. (In this photograph the larger bubbles are out of focus and therefore appear larger than they actually are). While these bubbles seem in the photographs to be similar to the vapor cavities observed in water, their action is much different. Once formed, these bubbles do not undergo the violent collapse associated with vapor bubbles, but gradually move upward as a result of buoyant forces. The stability of these bubbles indicates that they are gas-filled and probably form as a result of the coagulation of many small gas bubbles.

Gaseous cavitation in carbon tetrachloride, benzene, and acetone is very much like that observed in water. The bubbles migrate to the pressure nodes from which point they are buoyed upward. Small streamers are present at all times. Figure 11D shows a picture of the form of gaseous cavitation in carbon tetrachloride that is subject to low power inputs. At high power inputs the cavitation process differs considerably from that observed in water. The bubbles become extremely profuse and completely fill the entire liquid in the flask. Figure 12E is an example of this effect in benzene. In addition, two other phenomena are occurring. At the maximum level of power available, a streaming effect takes place. The liquid moves about in large vortices such that certain areas soon become clear of bubbles. This phenomenon is shown in Fig. 12F where a clear area in the benzene is forming at the focal point of the sound signal. In addition, in the case of acetone, if the hydrostatic pressure over the liquid is reduced and a strong sonic signal is applied, the profuse



A



B

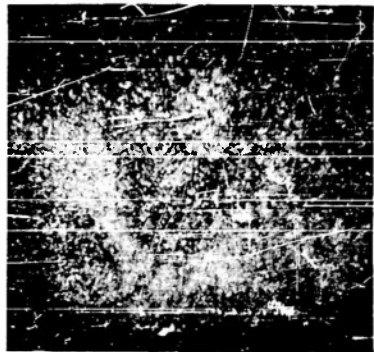


C

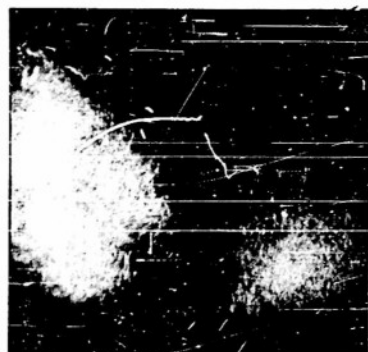


D

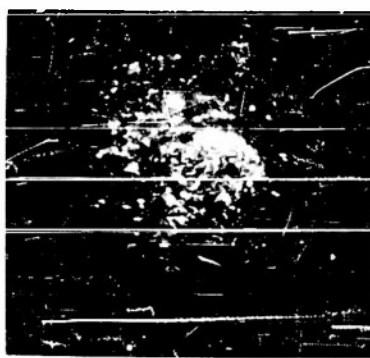
FIG.II. CAVITY AND BUBBLE FORMATION  
IN VARIOUS LIQUIDS



E



F



G



H

FIG. 12. CAVITY AND BUBBLE FORMATION  
IN VARIOUS LIQUIDS

cavitation phenomenon is occasionally preceded by a violent burst of bubbles, apparently vaporous cavitation bubbles, indicating a sudden release of strain energy.

In the more viscous liquids the form of gaseous cavitation is essentially the same as that observed in other liquids. In kerosene, a moderate sound signal produces profuse cavitation as shown in the picture of Fig. 12G while in olive oil, castor oil, and sperm oil it is much more difficult to produce profuse cavitation. Vortices or spiralling galaxies of bubbles can be created. Unfortunately the photographs do not capture the movement of this phenomenon. These galaxies usually consist of a large central bubble approximately 0.3 mm in diameter about which clusters of very small bubbles swirl. With the removal of the sound signal the vortex collapses and only the central bubble moves upward. The fine detail of the gas bubbles and the manner in which they are buoyed upward from pressure nodes is shown in Fig. 12H, illustrating gaseous cavitation in castor oil. Again the bubbles' diameters are approximately the resonant diameters, namely 0.1 mm.

Certain qualitative conclusions can be reached on the basis of these general observations. The bubbles in the majority of cases first appear at a pressure antinode. Occasionally, in the more viscous liquids, a bubble will appear at the center of a vortex. With the exception of these vortices, the bubbles immediately migrate in a nondescript manner to the pressure nodes. At these nodes the bubbles are either buoyed upward or coagulate to form a larger bubble prior to submitting to the buoyant forces. With the sole exception of water, profuse gaseous-type cavitation is possible in all liquids. This profuse cavitation is more readily observed in the lighter or less viscous liquids. On the other hand, true vaporous cavitation could be readily observed only in water. It therefore appears as though water differs from all other liquids examined in certain physical characteristics important to the process of gaseous cavitation. These characteristics will be discussed in the latter part of this chapter after a discussion of some quantitative data. But before proceeding to these quantitative data, one must examine the forces that are exerted upon the bubbles by the sound field. At high power inputs these

forces can become hopelessly complicated as a result of second order effects, the character of the focused sound signal, and the distortion of the sound field by the pulsating bubbles. In order to simplify matters, consideration will only be given to forces related to first and second order effects.

B. First and second order forces on gas-filled bubbles.

The principal forces that a gas bubble will experience in a sound field are the forces known as Bjerknes forces [46], [47]. These forces are based upon the principle of kinematic buoyancy which Bjerknes and his father first proposed. This principle, which is perfectly analogous to the Archimedian law, is that ([ 46] page 10) "any body which participates in the translatory motion of a fluid mass is subject to a kinetic buoyancy equal to the product of the acceleration of the translatory motion multiplied by the mass of water displaced by the body."

Suppose that a bubble is placed in a synchronously oscillating current or stream of fluid. It will be continually subject to a kinetic buoyancy; and, if the volume of the bubble is variable, it will experience a resultant force whose direction is that of the acceleration in the current at the time that the bubble has its maximum volume.

Mathematically, one can consider this force, called the Bjerknes force, in the following manner. The position of an element of a pulsating fluid can be written as .

$$\xi = \xi_0 + \xi_1 \sin \omega t$$

where  $\xi_c$  is the mean position of the element, and  $\xi_1$  is its maximum displacement. Suppose that there is within the fluid a bubble that displaces a mass of fluid given by the formula

$$M = \rho [v_0 + v_1 \sin (\omega t + \psi)]$$

where  $v_0$  is the mean volume of the bubble,  $v_1$  is the amplitude of the change in volume,  $\rho$  is the density of the fluid, and  $\psi$  is the phase angle between the pulsations of the bubble and the displacements of the fluid. In view of the principle of kinetic buoyancy the force,  $F$ , experienced by the bubble will be the product of the mass of the displaced fluid and the acceleration of the fluid. Thus

$$F = \rho [v_0 + v_1 \sin(\omega t + \psi)] [-\xi_1 \omega^2 \sin \omega t] .$$

The net or average force is

$$\bar{F} = -\frac{\rho \omega^2 v_1 \xi_1}{2} \cos \psi .$$

Thus the bubble will be subject to a force whose direction is that of the acceleration at the time when the bubble has its maximum volume.

The principle of kinetic buoyancy can be applied to the case of two pulsating bubbles. By means of similar analysis one can show that ([46] p. 32) "between two bodies pulsating in the same phase there is an apparent attraction; between bodies pulsating in the opposite phase there is an apparent repulsion, the force being proportional to the product of the two intensities of pulsation, and proportional to the inverse square of distance." The mathematical derivation for this force between two pulsating spheres in an incompressible fluid has been given by Basset [48] who obtained the approximate formula that

$$\bar{F} = -2\pi \frac{\omega^2 a^2 b^2 \alpha \beta \cos \omega t}{d^2} ,$$

where

$$a = \bar{a} + \alpha \sin \omega t = \text{radius of first sphere}$$

$$b = \bar{b} + \beta \sin \omega(t - \epsilon) = \text{radius of second sphere}$$

$$d = \text{distance between centers.}$$

Thus two spheres which pulsate at the same frequency will attract one another if their phases differ by less than  $90^\circ$  and repel one another if their phases differ by more than  $90^\circ$  and less than  $270^\circ$ . This force, called the Bernoulli force, is inversely proportional to the square of the distance between particles and is often very small though it will tend to coagulate adjacent bubbles whose pulsations bear the proper phase relations.

The concept of the Bjerknes force can be extended to the case of a small bubble that is immersed in a fluid and subject to an ultrasonic field. If the bubble's dimensions are much less than a wavelength, the bubble will participate in the motion of the fluid's particles while its volume will undergo changes in accordance with the pressure variation

of the sound field. If the bubble is in a free progressive wave the net force upon it will be zero since,

$$\phi = \phi_0 \cos \omega(t - \frac{x}{c}) .$$

and

$$F = \rho [v_0 + v_1 \sin \omega(t - \frac{x}{c})] [-\frac{\phi_0 \omega^2}{c} \cos \omega(t - \frac{x}{c})] .$$

Thus,

$$\bar{F} = 0.$$

In a standing wave system the situation is quite different. For example, if the bubble pulsates in phase with the sound signal,

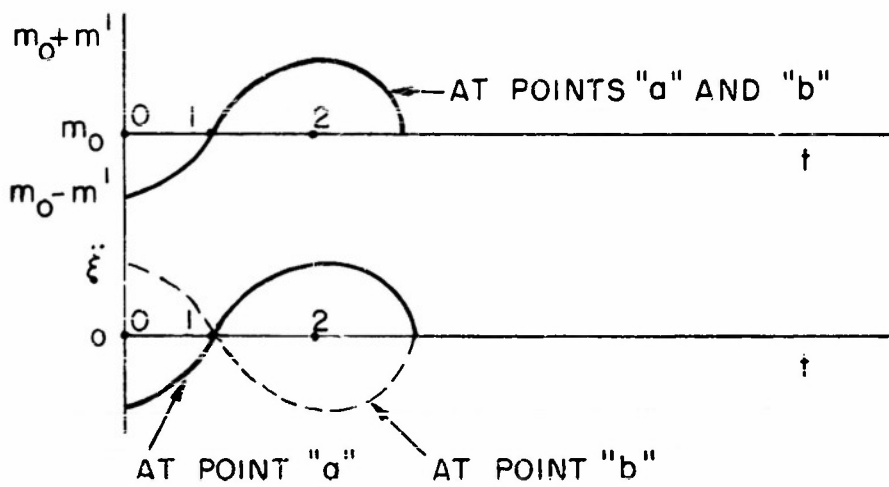
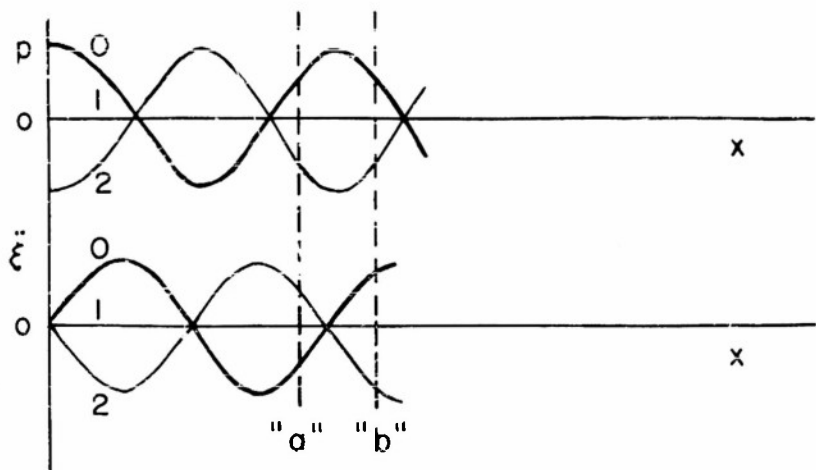
$$F = \rho(v_0 - v_1 \cos \omega t \cos \frac{\omega x}{c}) (A \cos \omega t \sin kx),$$

or

$$\bar{F} = -\frac{\rho v_1 A}{2} \cos \frac{\omega x}{c} \sin \frac{\omega x}{c} .$$

The bubble will migrate to the point at which  $\bar{F} = 0$ , namely, the pressure nodes or antinodes of the system. But, as will be shown graphically, at a pressure node the bubble will be in unstable equilibrium, while at a pressure antinode the bubble will be in stable equilibrium. If the bubble pulsates out of phase with the signal, the situation is reversed. A graphic picture of the physical process will clarify this problem. Figure 13 shows the pressure distribution at various times, 0, 1, and 2, and the corresponding distribution of the acceleration experienced by a parcel of fluid. The amount of additional fluid displaced by a bubble pulsating in phase with the applied sound signal is the negative of the pressure distribution multiplied by some constant. Figure 13 shows the manner in which the displaced mass and its acceleration will vary with time at points "a" and "b". There is obviously a net force at either point toward the pressure antinode, and the pressure node is a point of unstable equilibrium.

Having seen how these first order forces can account for the presence of bubbles at the pressure nodes or antinodes of a standing wave system one must consider the effect of the higher order terms of the large signal wave equation. The additional forces are extremely complicated and will only be outlined in this section.



$p$  = PRESSURE

$\xi$  = PARTICLE ACCELERATION

$m$  = MASS OF DISPLACED FLUID

$x$  = DISTANCE COORDINATE

$t$  = TIME COORDINATE

FIGURE 13.

Extensive studies regarding the large signal wave equation in non-viscous liquids have been given by Westervelt [49], [50], and in viscous liquids by Eckart [51]. In general, a particle or bubble in a liquid will be subject to four additional forces resulting from acoustical signals of large amplitude. As a result of momentum transfer a particle will be subject to a radiation pressure. As a result of the non-linear properties of the medium a particle will undergo a Stokes-type force which is in a direction opposite to that of the radiation pressure. Westervelt has shown that these two forces will tend to cancel themselves out, and in the case of bubbles, they will be neglected. A third force results from the asymmetry of the sound velocity field in the medium. As a result of this asymmetry, higher harmonics of the initial signal are present, and these harmonics result in a net force called the Oseen-type force. Finally, if the medium is viscous, rotational vortices can be established in the liquid. Eckart has shown that these vortices will be generated at the edge of the sound beam and will depend upon the viscosity of the liquid for their existence but not for their magnitude. The pressure at the center of a rotational vortex is  $P_o - (\omega^2 r_o^2 \rho)/2$ , where  $P_o$  is the pressure at  $r = r_o$ ,  $\omega$  is the angular velocity, and  $\rho$  is the density. There is, therefore, the possibility that a bubble will appear at the center of the vortex while smaller bubbles swirl about it in the circulation of the vortex.

Although the Oseen forces upon particles may become appreciable at very high sound intensities, they vary considerably and do little to explain the appearance of bubbles at antinodes. Once again one must look to the Bjerknes forces for the explanation. For a steady-state standing wave, Westervelt has shown that the particle displacement in Lagrangian coordinates is

$$\xi = \xi_o \sin\left(\frac{\omega x}{c_o}\right) \sin \omega t + \frac{\omega \xi_o^2}{8c_o} \left(\frac{y+1}{2}\right) \sin \frac{2\omega x}{c_o} = A + B \sin \omega t,$$

assuming the proper boundary conditions. The force upon a bubble in phase with the sound signal is, in Eulerian coordinates,

$$F = \rho(v_o - v' \frac{P}{P_o}) \ddot{\xi} = -(v_o - v' \frac{P}{P_o}) \frac{\partial P}{\partial x}$$

To transform to these coordinates Westervelt gives the relationship

and

$$P = \gamma P_0 \left\{ -\frac{\partial \xi}{\partial x} + \left(\frac{\gamma+1}{2}\right) \left(\frac{\partial \xi}{\partial x}\right)^2 + \xi \frac{\partial^2 \xi}{\partial x^2} \right\} ,$$

$$\frac{\partial P}{\partial x} = \gamma P_0 \left\{ -\frac{\partial^2 \xi}{\partial x^2} + (\gamma+2) \frac{\partial \xi}{\partial x} \frac{\partial^2 \xi}{\partial x^2} + \xi \frac{\partial^3 \xi}{\partial x^3} \right\} .$$

Then,

$$\begin{aligned} F &= -\gamma P_0 \left\{ v_0 - v' \gamma \left[ \frac{\gamma+1}{2} A_x^2 - A_{xx} + AA_{xx} + ((\gamma+1)A_x B_x - B_x + AB_{xx} + BA_{xx}) \sin \omega t \right. \right. \\ &\quad \left. \left. + \left( \frac{\gamma+1}{2} B^2 + BB_{xx} \right) \sin^2 \omega t \right] \right\} \left\{ (\gamma+2)A_x A_{xx} - A_{xx} + AA_{xxx} \right. \\ &\quad \left. + ((\gamma+2)A_x B_{xx} + (\gamma+2)B_x A_{xx} - B_{xx} + AB_{xxx} + BA_{xxx}) \sin \omega t \right. \\ &\quad \left. + ((\gamma+2)B_x B_{xx} + BB_{xxx}) \sin^2 \omega t \right\} \\ &= -\gamma [L + M \sin \omega t + N \sin^2 \omega t] [Q + R \sin \omega t + S \sin^2 \omega t] . \end{aligned}$$

Taking averages,

$$\frac{F}{\gamma} = LQ + \frac{LS+MR+NQ}{2} + \frac{3NS}{8} .$$

The average force is therefore an extremely complicated function.

At distances equal to any multiple of a half wavelength, however,

$$A = A_{xx} = B = B_{xx} = 0 = Q = R = S$$

and

$$\bar{F} = 0 .$$

Thus a point of equilibrium will still exist at the "antinodes" of the pressure wave. The pressure "nodes" will again be points of unstable equilibrium, for at distances equal to odd multiples of a quarter wavelength,

$$A = A_{xx} = B_x = B_{xxx} = 0 = M = Q = S ,$$

and

$$\bar{F} = 0 .$$

By using the formula for  $\bar{F}$  one could further speculate on the direction in which the bubble will move under various conditions. There can exist, for example, circumstances under which  $\bar{F} = 0$  at points that are neither pressure nodes or antinodes. The problem regarding the forces

on bubbles could well concern a thesis in itself. An analysis of the above equations suffices to indicate that the bubble can grow at a pressure anti-node even when the liquid is subjected to an intense sound signal.

C. A tabulation of the physical properties of the liquids examined.

It is rather unfortunate that no individual handbook of chemistry and physics provides a convenient tabulation of the physical properties of liquids. Because of this situation, Table I is provided. The data have been obtained from several sources to which reference is made. These tables are useful in the determination of parameters that are important to the phenomenon of cavitation.

Table I has been constructed on the basis of the following sources of information:

- (1) International Critical Tables, National Research Council, McGraw Hill, New York, 1933.
- (2) Physikalisch-Chemische Tabellen, Landolt-Bornstein, Springer, Berlin, 1933.
- (3) Taschenbuch für Chemiker und Physiker, J. D'Ans und E. Lax, Springerverlag, Berlin, 1949.
- (4) Handbook of Chemistry and Physics, C. D. Hodgman, Chemical Rubber Publishing Co., Cleveland, 1950.
- (5) Solubilities of Inorganic and Metal Organic Compounds, A. Seidell, D. Van Nostrand Co., New York, 1940.

In those cases where the solubility constant,  $a$ , was not given for atmospheric air itself, the constant was determined by assuming atmospheric air to be composed of 78.5 per cent nitrogen and 21.5 per cent oxygen. The diffusivity,  $D$ , has been determined by means of Arnold's [52], [53] equation:

$$D = \frac{B \sqrt{\frac{1}{M_1} + \frac{1}{M_2}}}{A_1 A_2 \mu_2 \left( V_1^{\frac{1}{3}} + V_2^{\frac{1}{3}} \right)^2}$$

where

$B$  = kinetic constant = 0.01 at 20° C

$M_1$  = molecular weight of solute = 28.97 gms for air (composition  
78.03% N<sub>2</sub>, 20.99% O<sub>2</sub>, 0.94% A, 0.03% CO<sub>2</sub>, 0.01% H<sub>2</sub>)

$M_2$  = molecular weight of liquid solvent

$A_1$  = abnormality factor = 1 for air

$A_2$  = abnormality factor = (4.70 for water  
(1.19 for acetone  
(1 for other liquids considered

$\mu_2$  = viscosity of liquid in centipoise

$V_1$  = molecular volume = 29.9 for air

$V_2$  \* molecular volume of liquid.

In addition to the above table the following additional information is useful (see Dalla Valla [ 26 ] p. 229 and Bikerman [ 23 ] p. 265):

Work of adhesion to a suspension of silica particles.

water	155.62	dynes/cm
-------	--------	----------

carbon tetrachloride	67.49
----------------------	-------

benzene	81.33
---------	-------

Heat of wetting to amorphous silica powder

water	64	joules/gm of dry material
-------	----	---------------------------

carbon tetrachloride	33.9
----------------------	------

benzene	33.9
---------	------

acetone	56.5
---------	------

to copper particles

castor oil	0.51
------------	------

kerosene	0.24
----------	------

to Floridin (a silicate)

kerosene	18.8
----------	------

Note: The work of adhesion and the heat of wetting indicate the degree of wetting of a solid by a liquid. Solid particles will be most stable in the liquid that best wets them. If one assumes that silica is the principal component in dust particles, the above figures are in agreement with the observations made in Chapter II with regard to the very high density of dust particles in water.

As a general reference and bibliography regarding all of the above properties see Partington [ 54 ].

TABLE I.

C. A tabulation of the physical properties of the liquids examined.

	$\rho$ $\frac{\text{gm}}{\text{cm}^3}$	$c$ $\frac{\text{m}}{\text{sec}}$	$\rho c \times 10^5$ $\frac{\text{gm}}{\text{cm}^2 \text{ sec}}$	$\sigma$ $\frac{\text{dynes}}{\text{cm sec}}$	$T_{B.P.}$ $^{\circ}\text{C}$	$P_v$ $\text{mm Hg}$	$\mu$ $\text{poise}$	$M$ $\frac{\text{gm}}{\text{dyne cm}}$	$a \times 10^{-12}$ $\frac{\text{mols}}{\text{dyne cm}}$	$D \times 10^{-5}$ $\frac{\text{cm}^2}{\text{sec}}$
acetone	0.79	1189	0.94	23.7	56.5	[ 184.8 612.6 ]	0.0033	58.08	6.28	6.25
kerosene	0.81	1324	1.07	28.0	~24.0	~0.01	0.04	~165(?)	~2.7	1.24
sperm oil	0.88	1440	1.27	~30	--	~0.01	[ 0.25 0.19 ]	165	~2.8	0.50
benzene	0.90	1170	1.05	28.9	80.0	[ 94 380 ]	0.0065	78.11	5.28	4.58
olive oil	0.92	1431	1.32	33.06	~28.6	~0.01	[ 0.84 0.36 ]	~282	3.0(?)	0.22
castor oil	0.97	1477	1.43	36.4	~26.5	~0.001	[ 6.3 2.3 ]	~298	~3.8	0.08
water	1.00	1440	1.44	72.8	100.0	[ 17.53 92.51 ]	0.01	18.02	0.75	1.95
methyl phthalate	1.18	1463	1.73	30(?)	282.0	~0.0001	0.178	194.18	3.0(?)	0.64
carbon tetrachloride	1.60	926	1.48	26.8	76.0	[ 91.0 317.1 ]	0.0098	153.84	7.08	3.22

 $\rho$  = density $c$  = velocity of sound $\rho c$  = specific acoustic impedance $\sigma$  = surface tension at  $20^{\circ}\text{C}$  $T_{B.P.}$  = boiling point $P_v$  = vapor pressure at  $20^{\circ}\text{C}$ . For the more volatile liquids the upper figure is  $P_v$  at  $20^{\circ}\text{C}$ ; the lower figure is  $P_v$  at  $50^{\circ}\text{C}$ . $M$  = molecular weight $a$  = solubility constant for air at  $20^{\circ}\text{C}$  $D$  = diffusivity of air in the liquid at  $20^{\circ}\text{C}$ 

$\mu$  = viscosity at  $25^{\circ}\text{C}$ . For the more viscous liquids the upper figure is  $\mu$  at  $25^{\circ}\text{C}$ ; the lower figure is  $\mu$  at  $40^{\circ}\text{C}$ .

D. The quantitative results.

Two types of measurements were sought by means of the measuring apparatus. As a first objective, measurements on gaseous cavitation in the interior of a liquid at a point remote from any surface were desired. And as a second objective, it was desired to obtain measurements on gaseous cavitation occurring upon a solid surface. It was naturally expected that the first set of measurements would prove to be the most difficult. The outcome of these observations, however, was far from satisfying. Fortunately, the success in obtaining the second objective more than compensated for the difficulty encountered in producing cavitation within the body of a liquid. But before proceeding to a more detailed discussion of these observations, the manner in which the liquids were kept saturated with air must be considered.

The most important requirement on any measurement of gaseous cavitation is that the amount of gas absorbed by the liquid must be known. In this experiment, the liquids were completely saturated with air before any measurements were made on them. The advantages of using gas-saturated liquids are twofold. By using the closed system described in Chapter III there is no need to resort to elaborate procedures in order to determine the gas content of the liquid, and gaseous cavitation can be more readily obtained in liquids that are fully rather than partially saturated with gas. Future plans, however, call for a system whose gas content can be regulated and measured. Such a system will necessarily be very complicated. In this experiment the technique used to saturate the liquids is as follows. A flask containing the liquid to be observed is connected to the flask support. The entire support is fastened securely in place, and the cavitation tank is filled with distilled water which is degassed and serves as the acoustical coupling medium between the transducers and the flask. By means of regulating valves the air pressure over the liquid is set to any desired amount. As the air pressure is increased or decreased a certain amount of air will be absorbed or evolved by the liquid, but the liquid will still be undersaturated or supersaturated with the gas in question. The mechanical agitator unit is set into operation, and the pressure over the liquid is plotted as a function of time. Eight typical curves showing the manner in which gas is absorbed or

evolved are illustrated in Fig. 14. The final equilibrium pressure over the liquid represents the pressure at which the liquid is completely saturated with air. As shown by the curves this condition is rapidly reached, and additional agitation of the liquid at a later time results in no change in the equilibrium saturation pressure. With sufficient experience one is able to estimate the initial pressure required at the commencement of agitation such that a desired equilibrium pressure will result. The success of the apparatus in obtaining saturation conditions is amply illustrated by the curves of Fig. 14.

Once saturation conditions have been obtained there is a waiting period of one to four hours (the more viscous liquids require the longer period) so that the gas bubbles within the liquid will either redissolve or be buoyed upward. The waiting time required by a liquid can be easily determined by measuring its cavitation threshold. In general, a period of four hours is more than ample for all of the liquids studied; that is, a waiting period of 24 hours gives no better results than a period of four hours. The liquid is then ready for the application of the ultrasonic signal.

As stated above the determination of the threshold for gaseous cavitation within the body of a liquid proved difficult if not impossible. At first, cavitation (observed visually) was obtained in all of the liquids tested. The net result of more than a hundred measurements was that with the sole exceptions of water and methyl phthalate, the walls of the container were serving as the initial sources for gaseous cavitation nuclei. Finally, when the containers were very carefully cleaned in the manner described in the previous chapter, it was possible to attain a situation whereby it was impossible with the maximum peak sound pressure (approximately 14 atmospheres) available with the equipment, to obtain gaseous cavitation in any of the liquids except water and methyl phthalate. This situation of being not liable to cavitation represents an optimum condition, for once any weak point such as a small bubble at the wall of the container appeared, the liquid would burst into profuse cavitation. Inasmuch as both water and methyl phthalate could be cavititated it was decided to make some measurements on them.

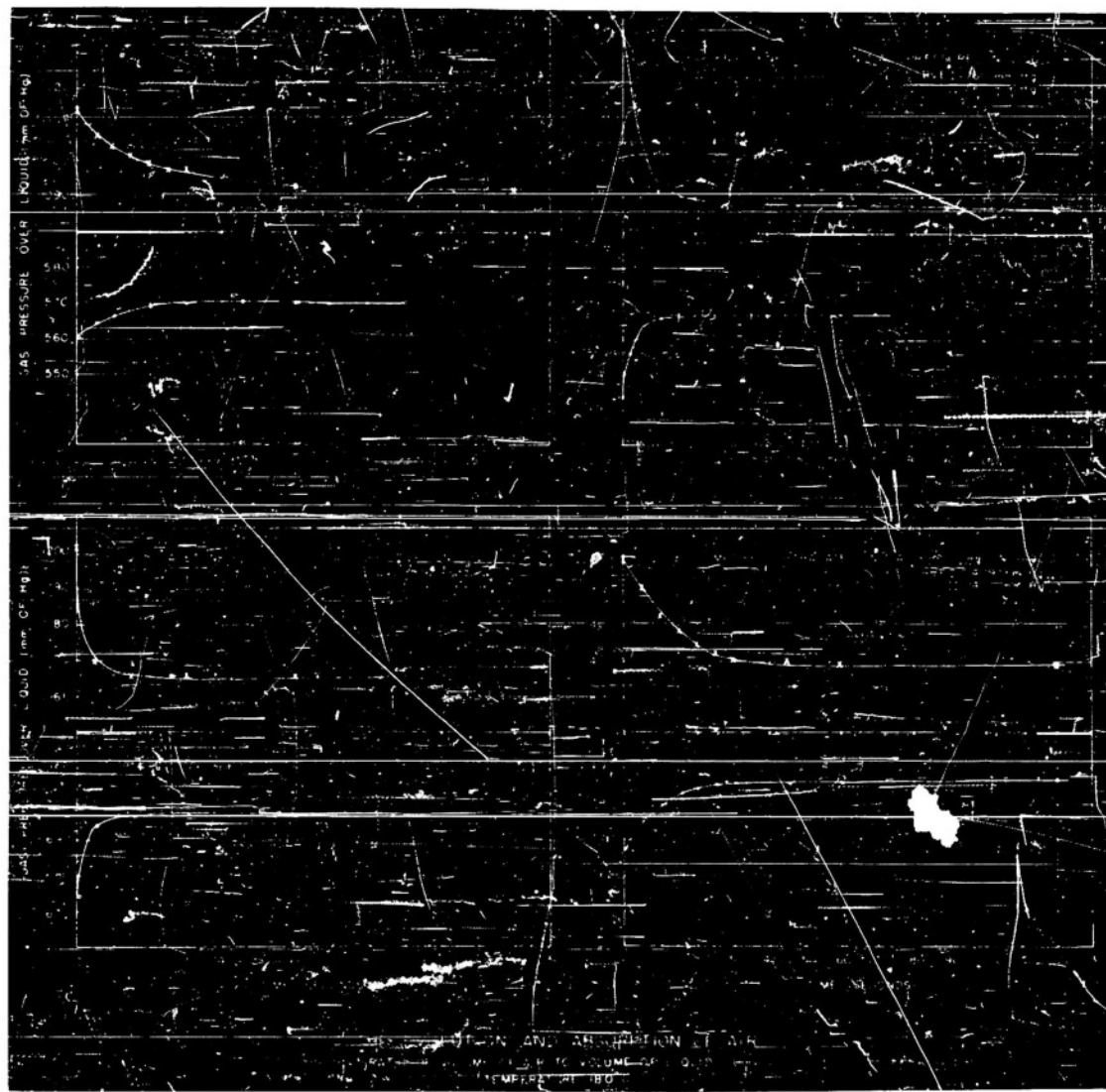


FIGURE 14

In order to determine a reading representative of the gaseous cavitation threshold for water or methyl phthalate several measurements were made. The input current to the driving elements was increased until cavitation could be observed visually. Four hours later the measurement would be repeated or a new measurement would be taken at a different saturation pressure. Several calibration runs using the probe hydrophone would be made during the period of measurement so that the pressure at the focus was known as a function of the input driving current. The final presentation of these measurements is shown in Fig. 15, the graph of cavitation threshold as a function of the hydrostatic pressure. With hydrostatic pressures greater than one atmosphere the threshold increases in a manner that is expected. But with hydrostatic pressures less than one atmosphere the threshold shows an increase rather than an expected decrease. It is felt that this increase in the cavitation threshold is due to the decrease in the size of the cavitation nucleus when there is in the liquid less gas available for diffusion into the nucleus during its incipience. This process has been discussed in Chapter II and will be substantiated in Chapter V.

The above measurements naturally led to a second set of observations on the occurrence of gaseous cavitation at the surface of a solid. Cavitation can be produced much more readily at a solid surface. Hence several liquids of differing viscosities can be studied. By using a probe hydrophone as the solid, the cavitation threshold can be detected electronically and with considerable accuracy in comparison with visual techniques. The theory of gaseous cavitation is equally applicable at the surface of a solid body as it is applicable at the surface of suspended particles. In fact, one of the principal situations in which cavitation is experienced is at a solid surface, for example, the face of a driving element. The only other extensive series of measurements on cavitation is that of Briggs, Johnson, and Mason [19], whose observations have been suspected to be the result of gaseous cavitation at the surface of the crystal transducer. If similar results could be obtained for gaseous cavitation at the surface of a probe, this suspicion would be confirmed.

To obtain these measurements the following technique was adopted. The probe hydrophone was first washed in acetone and allowed to dry. It

was then placed in the liquid upon which measurements were to be made, for a wetting period of 24 hours. The liquid was previously saturated with air. While the input signal was gradually increased the amplitude and waveform of the output signal was observed. With the beginning of gaseous cavitation the output signal showed a small amount of distortion and its increase in amplitude became less. With a still further increase of the input signal, extensive distortion of the output signal took place, and its amplitude decreased rapidly. In the plot of output signal as a function of input signal, see for example Fig. 17, the point of inflection of the curve was taken as the threshold for gaseous cavitation. Steady-state measurements were made on all of the liquids specified in Chap. IV, Sec. C. Additional pulse measurements were taken on four of the liquids. A waiting period of two hours was allowed between measurements which were successfully repeated two to three times. The estimated accuracy of all of these measurements is approximately  $\pm 0.2$  atmospheres. Figure 16 is a graph of the steady-state threshold for gaseous cavitation as a function of the viscosity. Plotted on this graph are the data of Briggs, Johnson and Mason. Three experimental curves are drawn; the curve given by Briggs et al; the curve that best fits the data obtained in this experiment; and the mean of these two previous curves. Both sets of data show the same trend and correlate very well. Thus it appears that the experimental observations of Briggs et al refer to gaseous cavitation. Figures 17, 18, 19, and 20 are graphs of pulse length effects in liquids. These measurements will prove very useful in the theoretical discussion presented in Chapter V. The points at which these curves deviate from the linear curves shown are taken as the thresholds for gaseous-type cavitation corresponding to various pulse lengths. These thresholds increase with a decrease in pulse length only if the duration of the applied signal is less than a specific value (defined as the minimum pulse length). For signals whose duration is greater than or equal to the minimum pulse length the threshold for gaseous-type cavitation is the same as the steady-state threshold. Figure 21 is a graph of this minimum pulse length as a function of viscosity. An experimental curve that best fits these points has been drawn.

#### E. Some qualitative conclusions regarding gaseous cavitation.

Water and methyl phthalate turned out to be the only liquids studied in which gaseous cavitation could be produced without the presence of a foreign

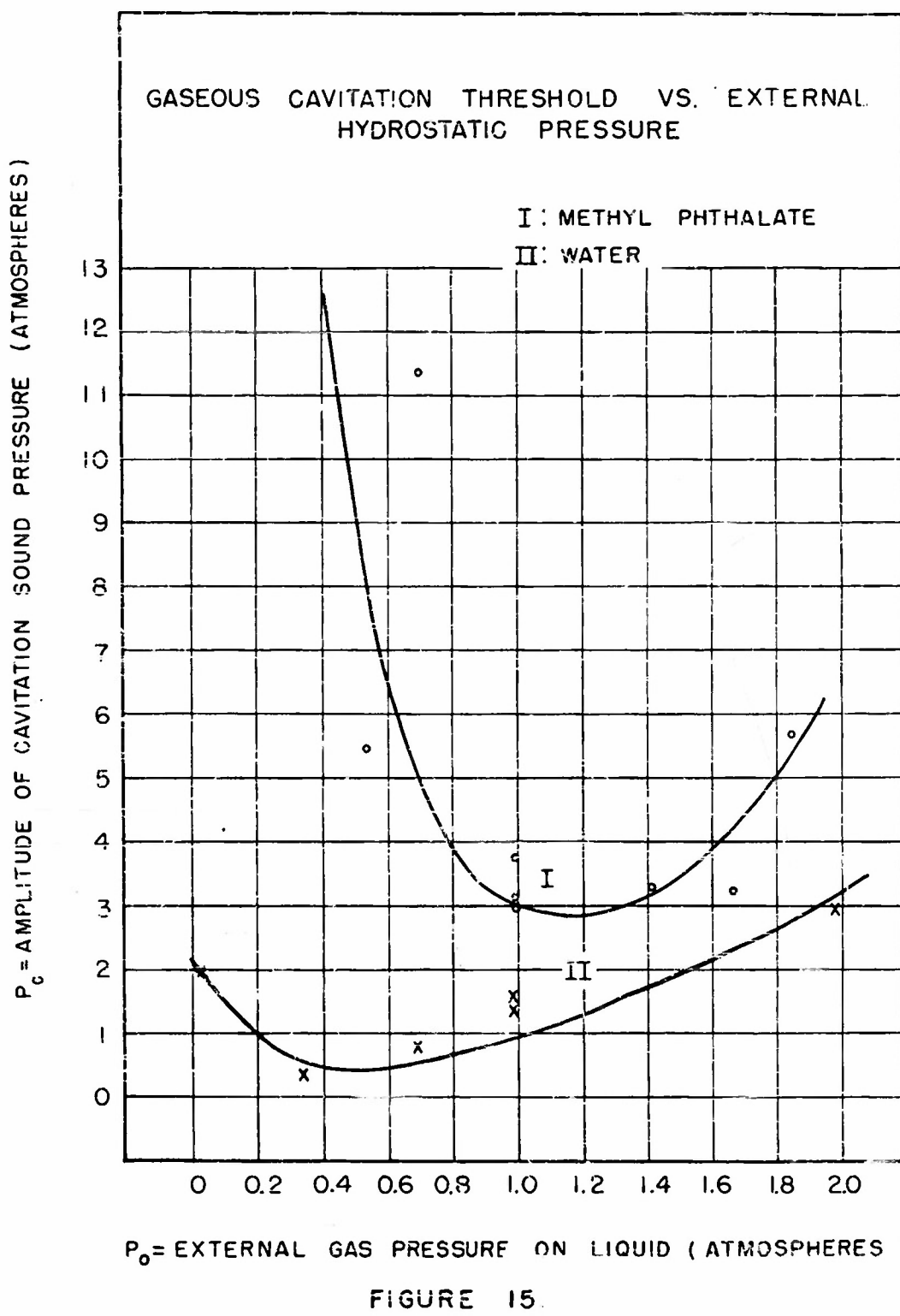
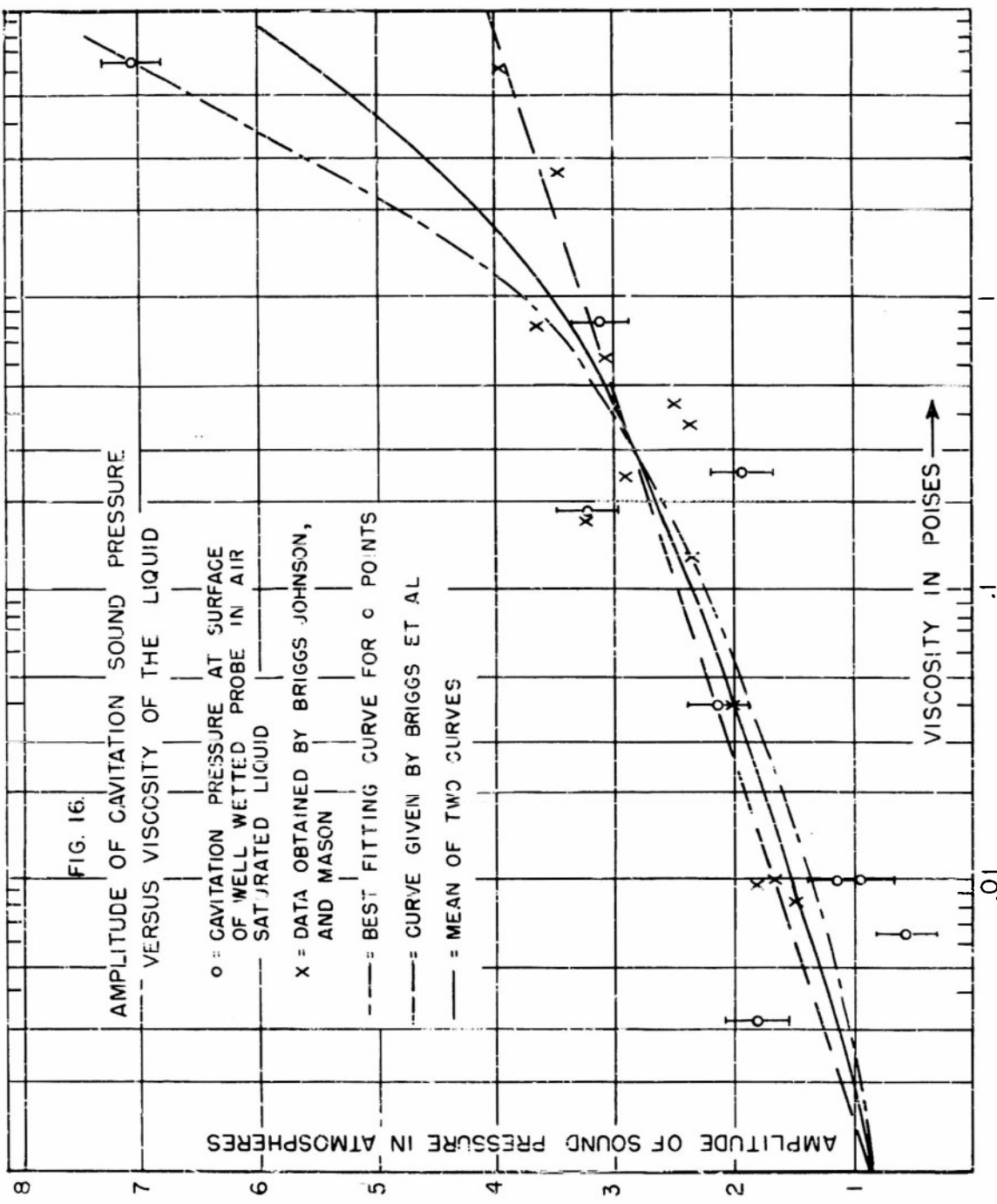


FIGURE 15.



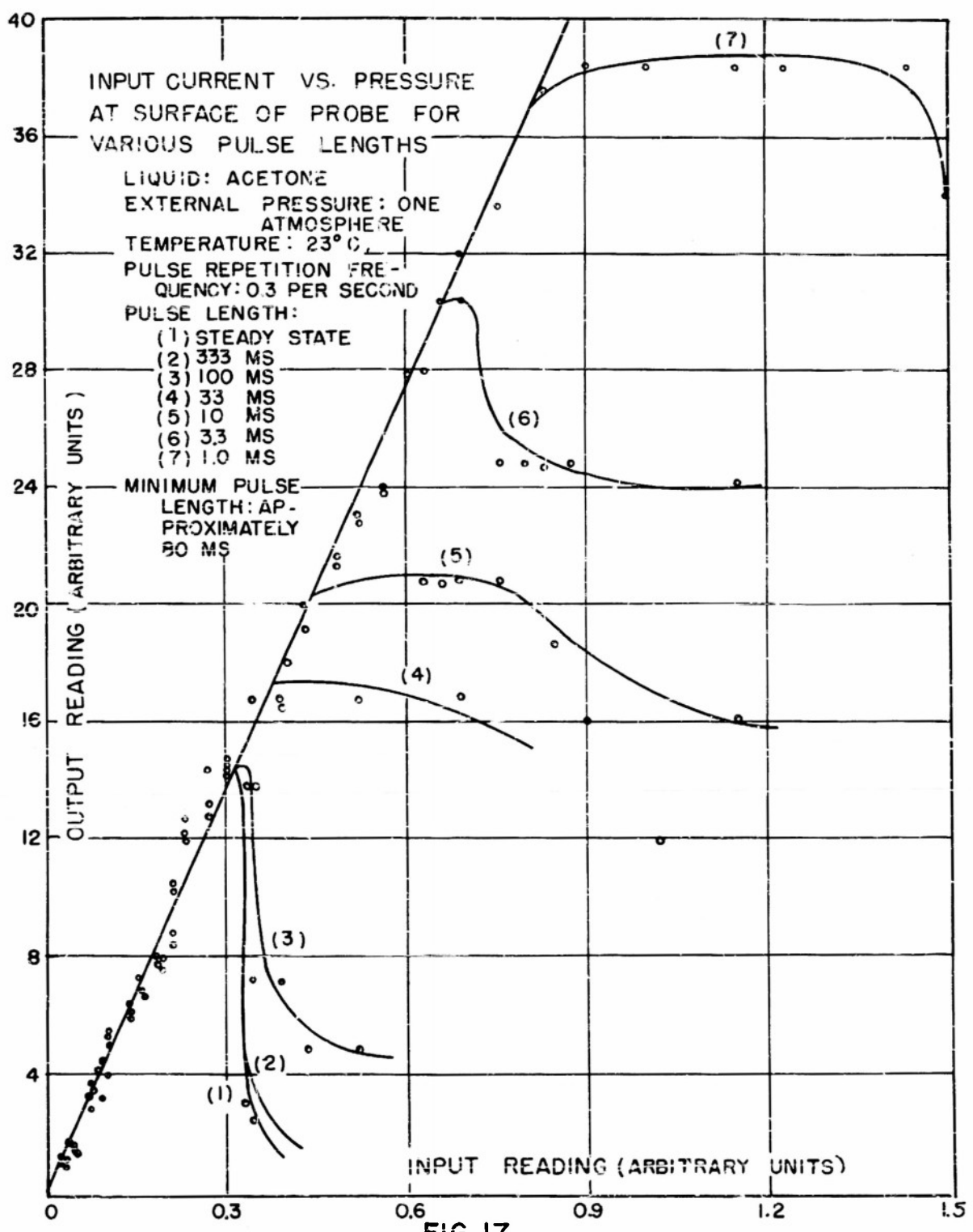


FIG.17.

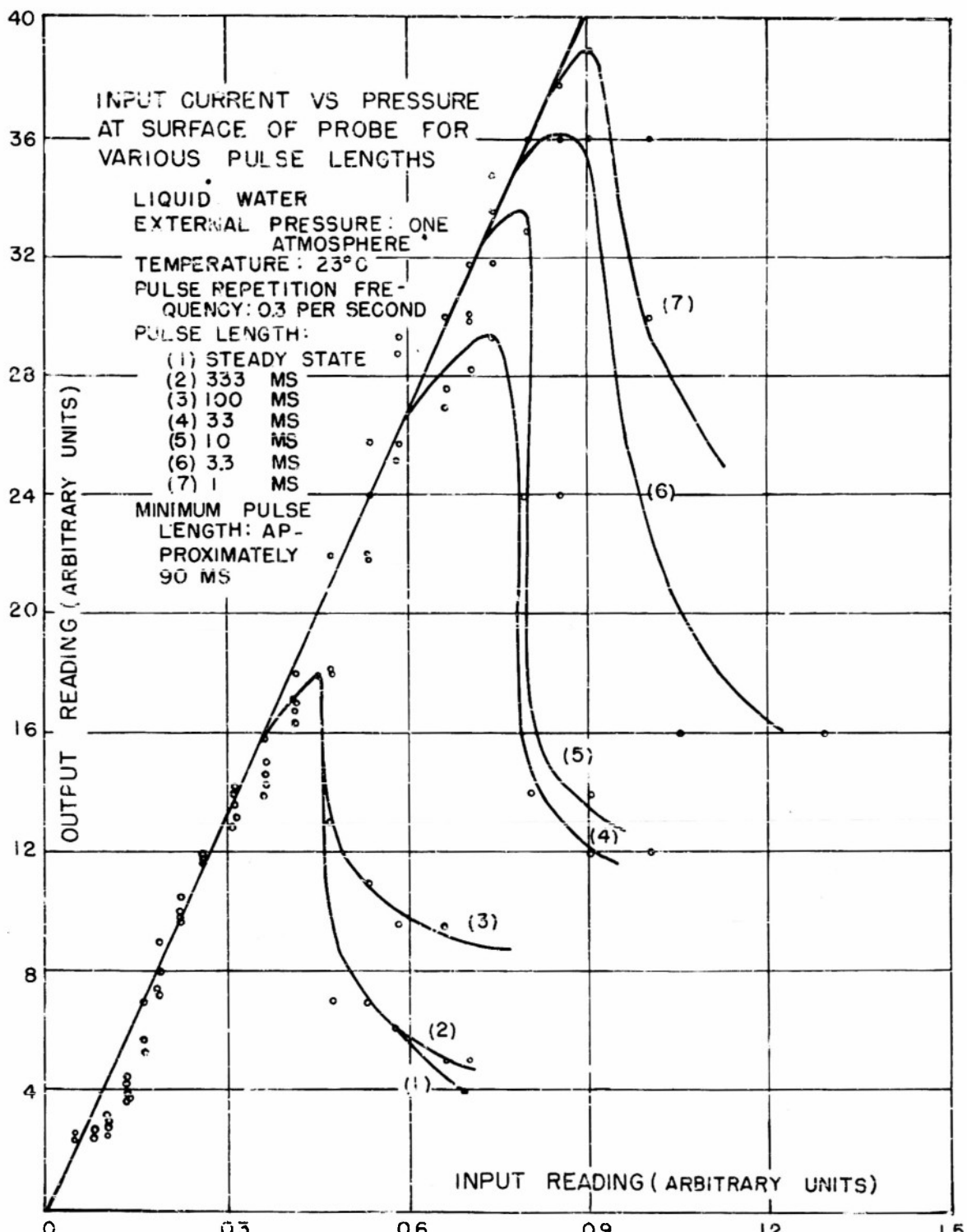


FIGURE 18.

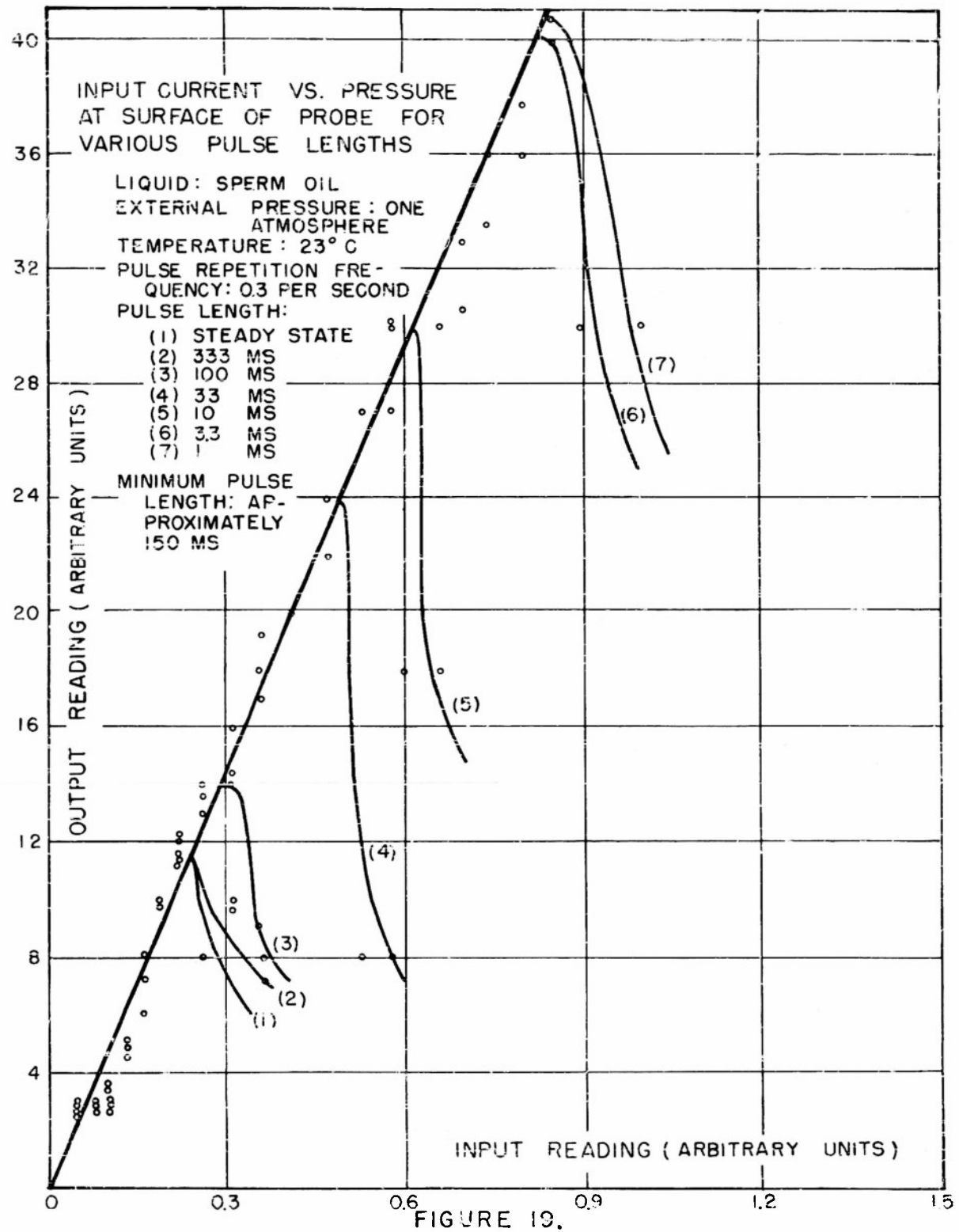


FIGURE 19.

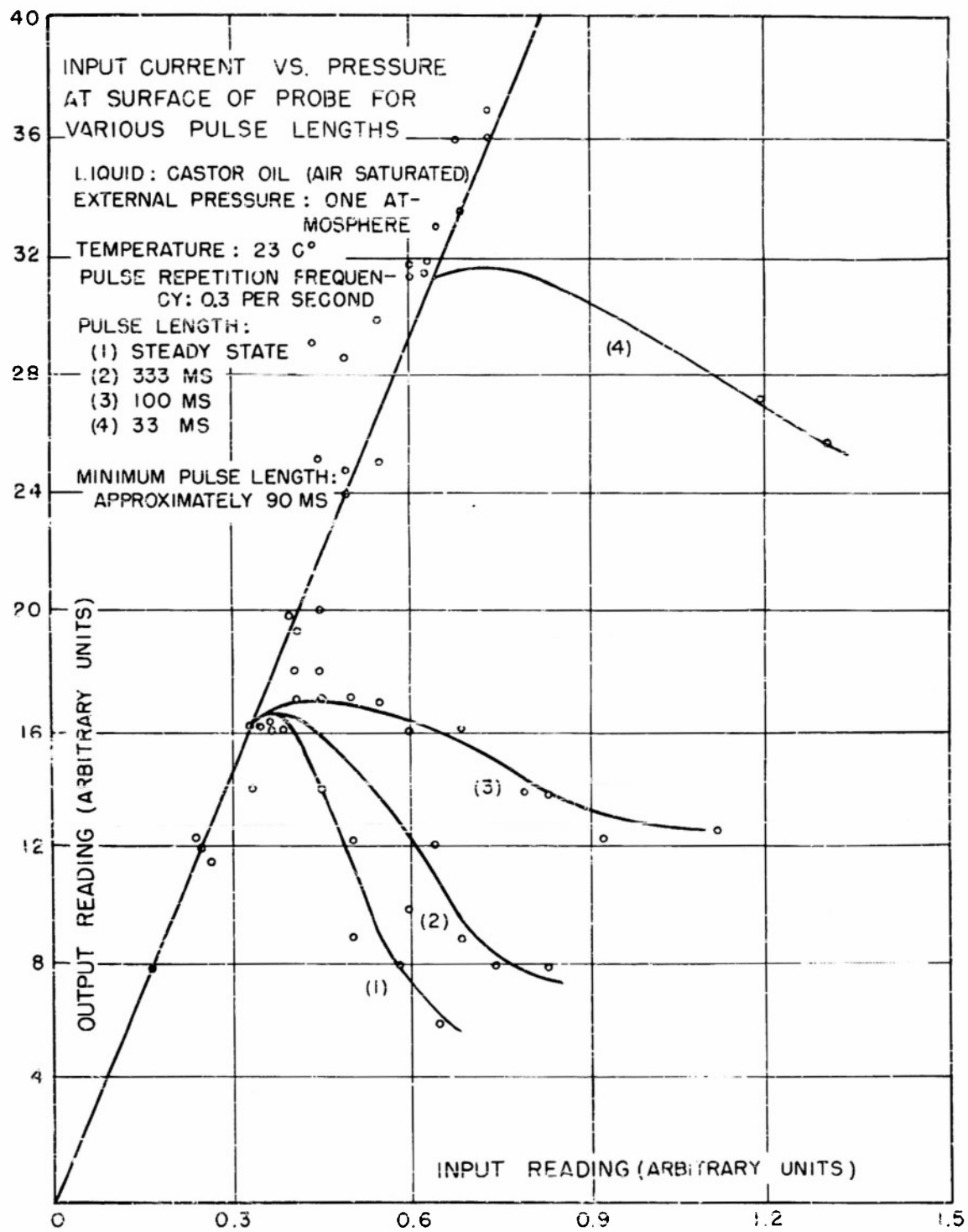
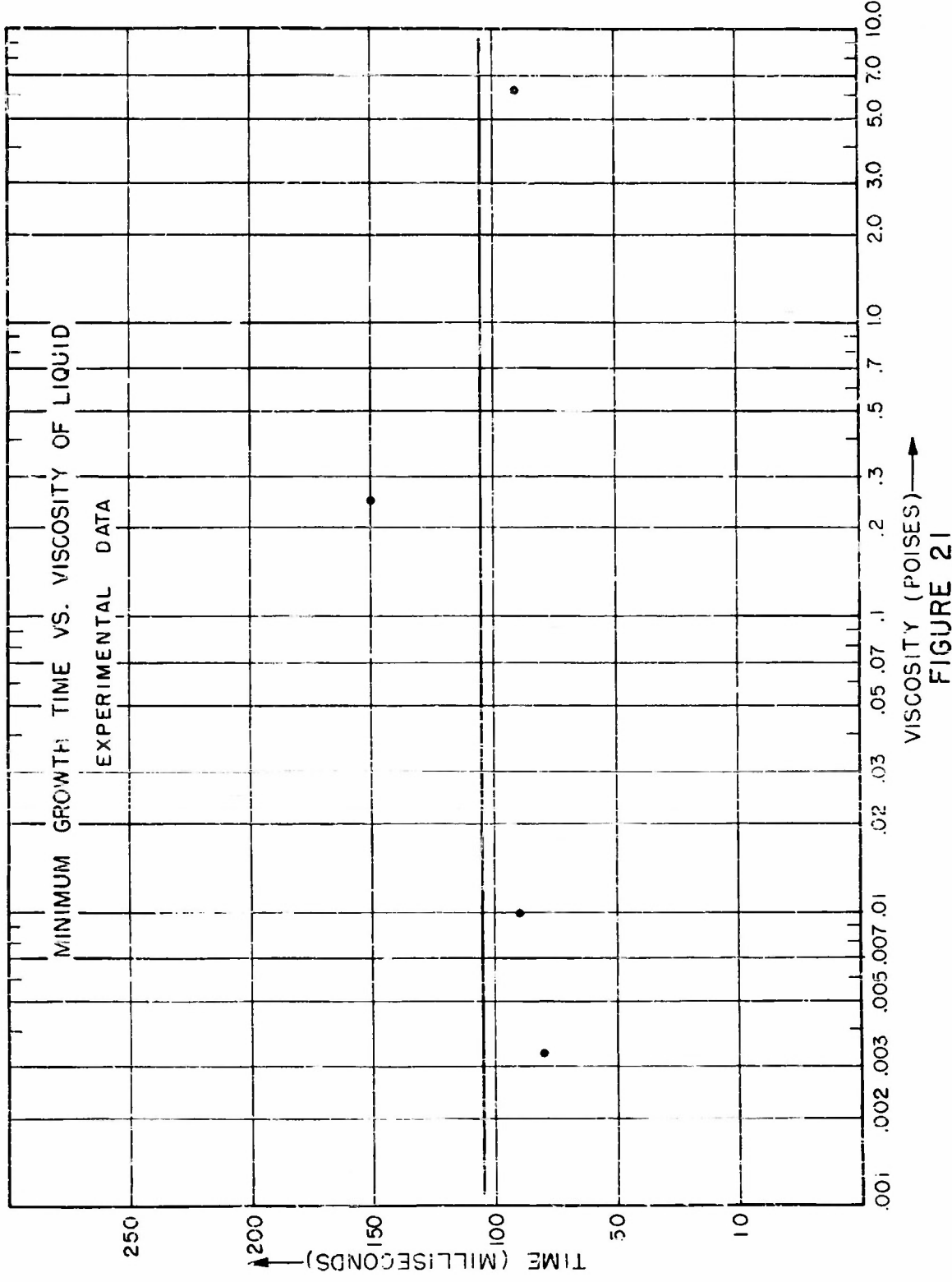


FIGURE 20



solid body. Examination of the physical properties of the liquids tested shows that the only common property of water and methyl phthalate in contrast to the other liquids is their great affinity for dust particles. It appears, then, that those liquids which exhibit the greatest work of adhesion for dust particles will most probably have the proper particulate matter in sufficient size distribution to serve as sources for the cavitation nuclei.

For all of the liquids studied, profuse cavitation was obtained least readily in water. Compared to the other liquids, water has very anomalous properties. It has from one third to one tenth of the solubility and almost three times the surface tension of the other liquids studied in this experiment. On the basis of this observation it appears that the profuseness of gaseous cavitation will be a function of the gas solubility (and perhaps the surface tension) of a liquid.

In conclusion, one is able to predict that if the particulate matter present in a liquid could be removed, the threshold for cavitation, gaseous or vaporous, would rise dramatically. The method for accomplishing this result must await future research.

## V.

### COMPARISON BETWEEN THEORY AND EXPERIMENT

#### A. The threshold for rectified diffusion.

The concept of rectified diffusion is discussed in reference [27]. This concept is based upon the manner in which a gas-filled bubble pulsates when subject to an acoustic signal. If the bubble is below resonant size (see reference [27]), the radius of the bubble will decrease during the positive half-cycle of the applied signal. The pressure of the gas within the bubble will be greater than the gas tension within the liquid such that gas will diffuse out of the bubble and into the liquid. During the negative half-cycle of the applied signal the bubble will expand. The situation will be reversed, and gas will diffuse into the bubble which is undersaturated with respect to the liquid. But the surface area of the bubble will be greater for the half-period during which there is an influx of gas, and more gas will diffuse into the bubble than outward during its pulsation cycle. Hence there will be a

net sound-induced diffusion of gas into the bubble. For bubbles greater than resonant size the process will be essentially the same except that the pulsations of the bubble will be out of phase with the applied sound signal. If the rate of this net influx exceeds the rate at which gas leaves the bubble as a result of the internal excess pressure due to surface tension, the bubble will grow. This process of growth is called "rectified diffusion."

In reference [27], equations (4)-(18), the threshold for gaseous-type cavitation,  $A_{\infty}$ , was defined by the condition that the average number of moles of gas entering or leaving the bubble shall be zero. If the amplitude of the applied sound signal is greater than  $A_{\infty}$  for a nucleus of radius  $R_o$ , the bubble will grow as a result of the rectified diffusion of gas. The formula obtained for  $A_{\infty}$  is

$$A_{\infty} = \sqrt{\frac{2(P_o + \frac{2\sigma}{R_o} - g_o) \omega^2 R_o^2 (U^2 + V^2) \sqrt{\alpha^2 + \beta^2}}{3\gamma(P_o + \frac{2\sigma}{R_o}) (\cos \ell - \sin \ell)(1 + 2R_o \sqrt{\frac{\omega}{2D}})}}$$

where

$P_o$  = hydrostatic pressure

$\sigma$  = surface tension

$R_o$  = radius of bubble

$\omega$  = angular frequency

$\gamma$  = specific heat of gas within bubble

$D$  = diffusion constant

$\alpha, \beta$  = heat conduction parameters defined in TM25, reference [27], equations (2)-(20) and (2)-(24).

$\ell = \tan^{-1} \beta / \alpha$

$U, V$  = real and imaginary part of the impedance presented by a bubble to a sound wave. Defined in TM25, reference [27], equations (3)-(20).

The term,  $\sqrt{\omega/2D}$  in this equation, results from the fact that the diffusivity constant of the liquid is finite. This term can be shown to be proportional to the reciprocal of the wavelength of the diffusional wave in the fluid or proportional to the reciprocal of the velocity of the diffusional wave if the frequency is constant. Inasmuch as the diffusivity constant,  $D$ , is

proportional to the reciprocal of the viscosity, the diffusional wavelength will decrease with viscosity. But, for similar gas concentrations at the surface of the bubble, this decrease in wavelength will produce an increase in the concentration gradient at the surface of the bubble. This increase will favor a smaller value for  $A_{\infty}$  as indicated in the equation.

The above relation for  $A_{\infty}$  is very sensitive to the radius,  $R_o$ , of the nucleus. In comparing the experimental values of the threshold for gaseous-type cavitation with the theoretical values, a value for  $R_o$  will be chosen such that the theoretical value of  $A_{\infty}$  for one liquid will approximate the experimentally observed value. On the basis of this value for  $R_o$ , the theoretical values for  $A_{\infty}$  will be calculated for the remainder of the liquids that have been studied. However, the chosen value of  $R_o$  should be of the order of magnitude of  $10^{-5}$  cm to  $10^{-4}$  cm in accordance with the evidence presented in Chapter II. In addition, Blake's observations on vaporous cavitation in water indicated that  $R_o$  is of the order of magnitude of  $1.1 \times 10^{-5}$  cm. It will be shown in the next section that  $R_o$  is of these orders of magnitude and that good correlation can be obtained between the observed and predicted thresholds for gaseous-type cavitation if one additional assumption is made.

As a first approximation assume that the diffusivity constant is infinite, that is,  $D \rightarrow \infty$ . Upon taking  $g = P_o = 10^6$  dynes/cm<sup>2</sup>,  $R_o = 8 \times 10^{-5}$  cm, and  $\omega = 377 \times 10^3$  sec, one obtains the following values for  $A_{\infty}$ :

Table I

<u>Liquid</u>	<u>Cavitation Threshold (atmospheres)</u>	
	<u>Calculated</u>	<u>Observed (Mean Experimental Curve)</u>
acetone	1.8	1.2
kerosene	2.0	2.0
sperin oil	2.1	2.6
benzene	2.1	1.4
olive oil	2.3	3.4
castor oil	5.0	5.6
water	3.7	1.5
methyl phthalate	2.1	2.7
carbon tetrachloride	1.8	1.5

Considering the difficulty in making cavitation measurements the above first order theory shows excellent agreement with the experimental observations. It has been necessary to assume, however, that  $\frac{1}{D} \frac{\partial c}{\partial t} \approx 0$ . The next obvious step in this analysis is to consider the case where D is finite. This more precise analysis of the diffusion problem will lead to closer agreement with the experimental results only if certain additional assumptions are made. Many other physical variables will affect the above results. The effects of parameters, such as the manner in which each of the above liquids wets a surface or the receding and advancing contact angles within the crevice of a surface are unknown. A qualitative discussion of these factors has been given in Chapter IV. Other effects such as the variation of  $R_o$ , etc., will now have to be considered.

For a finite diffusivity constant, and for  $g = P_c = 10^6$  dynes/cm<sup>2</sup>,  $R_o = 3.5 \times 10^{-5}$  cm, and  $\omega = 377 \times 10^3$ /sec, one obtains the following values for  $A_\infty$ :

Table II

<u>Liquid</u>	<u>Cavitation Threshold (atmospheres)</u>	
	<u>Calculated</u>	<u>Observed</u>
acetone	1.6	1.2
kerosene	1.3	2.0
sperm oil	1.1	2.6
benzene	1.7	1.4
olive oil	1.0	3.4
castor oil	1.2	5.6
water	2.9	1.5
methyl phthalate	1.1	2.7
carbon tetrachloride	1.6	1.5

The inclusion of a finite diffusivity constant breaks down the previous agreement (where  $D \rightarrow \infty$ ) between theory and experiment. This breakdown is a result of the greater concentration gradient at the surface of the bubble in those liquids that have smaller diffusivity constants. This effect over-compensates for the manner in which viscosity reduces the amplitude of the pressure fluctuations within the bubble. The inclusion of a finite diffusivity constant, however, leads to closer agreement between the assumption of

radii for the cavitation nuclei of gaseous and vaporous cavitation. It appears that this more exact analysis represents a step in the proper direction if one can account for the poor agreement between the theoretical and observed values for the more viscous liquids. There are two possible assumptions that can be made to correlate the theoretical and experimental results. First one can assume that the nucleus radius,  $R_o$ , is a function of the diffusivity, D, such that the term  $R_o \sqrt{\frac{\omega}{2D}}$ , does not become too large for the highly viscous liquids. This assumption can be placed on a sound physical basis by reconsidering the discussion of cavitation nuclei in Chapter II. It has been shown that there are two ways in which cavitation nuclei are formed. Either (1) a sufficient amount of gas is stabilized within cracks of a dust particle so as to provide a weak point in the liquid; or, (2) the nucleus can form, de novo, at the bottom of a concave cavity if the liquid only partially wets the solid particle. In either case there will issue forth with the first sufficiently great negative peak of the applied sound signal a small bubble which has been designated the "cavitation nucleus." The size of this nucleus is  $R_o$  where  $R_o = R_1 + \Delta R$ . The term  $R_1$  represents the size of the nucleus if all the gas stabilized in the particle issued forth to form a cavitation nucleus. The term  $\Delta R$  is due to the additional amount of gas that diffuses into the nucleus as it issues forth from the cracks in the particle. Assume that  $\Delta R > R_1$ . If the cavitation nucleus is formed in the manner described in case (1) above, the term  $R_1$  will be essentially constant while the term  $4\pi R_1^2 \frac{\Delta R}{\Delta t} \propto \frac{\Delta m}{\Delta t}$ . But  $\frac{\Delta m}{\Delta t} = 4\pi R_1^2 D \left( \frac{\partial c}{\partial r} \right)_{r=R_1}$ . Thus  $\Delta R \propto D \left( \frac{\partial c}{\partial r} \right)_{r=R_1} \Delta t$ . But an expression has been obtained for  $\left( \frac{\partial c}{\partial r} \right)_{r=R_1}$ , and by considering this expression when  $\omega t = \frac{3\pi}{2}$  it is apparent that

$$\Delta R \propto a [D f(\sigma, \omega, \mu, A, R_1) + D^{1/2} g(\sigma, \omega, \mu, A, R_1)] .$$

If the cavitation nucleus is formed in the manner described in case (2) above, that is, de novo formation, both  $R_1$  and  $\Delta R$  will be proportional to  $a [D f(\sigma, \omega, \mu, A, R_1) + D^{1/2} g(\sigma, \omega, \mu, A, R_1)]$ . Finally, the transient variations of  $R_1$  as discussed in Chapter II, will further complicate the process, and favor the production of larger nuclei in the less viscous liquids. Assume, therefore, that  $R_o \propto \sigma a D^{1/2}$ . The calculated results for  $A_\infty$  then become:

Table III

<u>Liquid</u>	$10^5 R_o$ (cm)	Cavitation Threshold (atmospheres)	
		<u>Calculated</u>	<u>Observed</u>
acetone	8	0.7	1.2
kerosene	1.8	2.8	2.0
sperm oil	1.28	3.8	2.6
benzene	7.04	0.8	1.4
olive oil	1.	4.7	3.4
castor oil	0.80	5.8	5.6
water	1.64	7.9	1.5
methyl phthalate	1.55	3.1	2.7
carbon tetrachloride	7.29	0.7	1.5

With the sole exception of water which is anomalous with regard to surface tension, and gas solubility, the agreement between theory and experiment is excellent. Actually, the assumption that  $R_o \propto \sigma a D^{1/2}$  is not exact, yet it is felt that in view of the agreement between theory and experiment as well as its physical basis this assumption is well justified.

A second hypothesis that can be made is that there is an effective diffusional wavelength  $\lambda_{D_e}$ , greater than the actual diffusional wavelength,  $\lambda_D$ , in viscous liquids, where

$$\frac{\lambda_{D_e}}{2\pi} = \sqrt{\frac{2D_e}{\omega}}$$

and

$$\frac{\lambda_D}{2\pi} = \sqrt{\frac{2D}{\omega}}$$

The effect of  $\lambda_{D_e}$  will be to bring about a closer agreement between theory and experiment. It will be shown, however, that the reasoning regarding a physical basis for  $\lambda_{D_e}$  is not as tenable as that for the variation of  $R_o$ . One can consider the effective diffusional wavelength in the following manner.

Let  $A$  represent the area of the bubble, and  $V$ , the volume. The change in the number of gas mols inside the bubble is  $\delta m = \frac{V}{R*T} \delta p_g$ . During the positive half cycle of the applied signal, approximately  $\delta m$  mole of gas will

be removed from the bubble and vice versa. A fraction  $n$  of  $\delta m$  will diffuse to a depth of approximately  $\lambda_D$  cm in one half period. The maximum allowable change in the concentration of the mols of gas saturating the liquid is  $a\delta p_g$ . Hence,

$$\frac{n \delta m}{\frac{4\pi}{3} ((R_o + \lambda_D)^3 - R_o^3)} = \frac{n R_o^3 \delta p_g}{R * T ((R_o + \lambda_D)^3 - R_o^3)} = a \delta p_g ,$$

or

$$n = \frac{[(R_o + \lambda_D)^3 - R_o^3] a R * T}{R_o^3}$$

Suppose  $R_o = 3.5 \times 10^{-5}$  cm. Then, at  $T = 300^\circ A$ , one can list the following values for  $n$ :

Table IV

<u>Liquid</u>	<u><math>n</math></u>
acetone	$\geq 1$
kerosene	0.935
sperm oil	0.425
benzene	$\geq 1.$
olive oil	0.240
castor oil	0.147
water	0.405
methyl phthalate	0.570
carbon tetrachloride	$\geq 1.$

The remaining number of mols of gas, that is,  $(1-n)\delta m$ , will form a monomolecular or polymolecular layer on the inner surface of the bubble. The adsorbability of the liquid molecules for the gas molecules will be a function of both the binding forces between the liquid and gas molecules and the pressure exerted by the gas molecules. With maximum adsorption it will be assumed that each liquid molecule adsorbs one gas molecule. As an example take the extreme case of castor oil for which  $n = 0.147$ . Assume that  $A = 5$  atmospheres. The maximum excess number of mols is  $m'$ , where

$$n' \approx (1-0.147) \frac{\frac{4}{3} \pi R_o^3}{R \cdot T} A \left(1 + a_1 \frac{2\sigma}{R_o}\right)$$

$$\approx 39.6 \times 10^{-18} \text{ mols} = 2.38 \times 10^7 \text{ molecules.}$$

The area of a molecule of castor oil is approximately  $(7.1 \times 10^{-8})^2 \text{ cm}^2$ , or  $50 \times 10^{-16} \text{ cm}^2$ , and if each surface oil molecule adsorbs one gas molecule, the total area required by the molecules of gas will be approximately  $10^{-7} \text{ cm}^2$ . But the equilibrium area of a bubble whose radius is  $3.5 \times 10^{-5} \text{ cm}$  is  $0.154 \times 10^{-7} \text{ cm}^2$ , and this area will be reduced to about  $0.023 \times 10^{-7} \text{ cm}^2$  during the positive part of the pressure cycle. In order to adsorb at the surface of the bubble all of the excess gas molecules it is necessary to assume that few gas molecules are present in the surface layer when the bubble is of equilibrium size, and that a polymolecular layer, roughly 45 molecules thick is formed at the surface of the bubble during the peak of the positive pressure cycle. These assumptions are very extreme and highly subject to question. It seems reasonable, however, to assume that some molecules will be adsorbed at the surface of the bubble, and the net effects will be an effective diffusional wavelength,  $\lambda_{D_e}$ , that is greater than  $\lambda_D$ . Whether or not  $\lambda_{D_e}$  will be sufficiently large to bring about agreement between the theory and the experiment is doubtful. One can write, however, that the gas within the cavitation bubble will experience an effective diffusivity constant,  $D_e$ , such that

$$D_e = f(n', D, D', p_g) \approx [1 - n'(p_g)] D + n'(p_g) D' ,$$

where

$n'(p_g)$  = fraction of mols of gas that form a molecular layer on the inner surface of the bubble (a function of the gas pressure  $p_g$  and the binding forces between the liquid and gas molecules).

$D'$  = diffusivity constant of gas going to form the molecular layer.

$D$  = diffusivity constant of gas passing through a particular liquid.

As an example, take  $R_o = 3.5 \times 10^{-5} \text{ cm}$  and  $\lambda_{D_e}/2\pi = 1.80 \times 10^{-5} \text{ cm}$  for the more viscous liquids. The following results are then obtained:

Table V

<u>Liquid</u>	<u>Cavitation Threshold (atmospheres)</u>		<u>Diffusional Wavelength</u>	
	<u>Calculated</u>	<u>Observed</u>	$10^5 \frac{\lambda_D}{Z\pi}$ (cm)	$10^5 \frac{\lambda_{De}}{Z\pi}$ (cm)
acetone	1.6	1.2	1.821	1.821
kerosene	1.8	2.0	0.811	1.80
sperm oil	2.4	2.6	0.515	1.80
benzene	1.7	1.4	1.558	1.558
olive oil	2.2	3.4	0.342	1.80
castor oil	3.1	5.6	0.206	1.80
water	2.9	1.5	1.018	1.018
methyl phthalate	1.9	2.7	0.583	1.80
carbon tetrachloride	1.6	1.5	1.309	1.309

A graph of all of the above theoretical results and the mean experimental curve is shown in Fig. 22. The agreement between the observed results and those calculated on the basis of an effective diffusional wavelength is certainly not as good as that obtained by taking into account the variation of  $R_o$ . Nor is the physical basis for  $\lambda_{De}$  as acceptable as that for the variation of  $R_o$ .

In order to study further the hypothesis regarding a variation of  $R_o$ , additional experiments must be devised. A careful determination of the functional relationship between the threshold for gaseous-type cavitation and frequency is highly desirable. Unfortunately the transducers used in the experiment described in this memorandum are resonant elements, nor was the equipment constructed for measurements with frequency as a variable parameter. An additional measurement of importance is that of the finite growth time of the gaseous-type cavitation bubbles, inasmuch as their growth time is implied in the theory of growth by means of rectified diffusion. The functional relationship between the radius of the bubble and time is exceedingly complicated and as yet undetermined, although approximate calculations can be made [55]. Its solution will obviously require step-by-step machine computations (see ref. [27]). Although the data presented in this memorandum indicate a constant growth time of approximately  $10^{-5}$  milliseconds, more experimental data and theoretical work are required.

**B. Summary.**

In this chapter good agreement has been established between the theoretical and experimental values for the thresholds for gaseous-type cavitation. This agreement is based upon the hypothesis that the radii of cavitation nuclei satisfy a certain functional relationship, that has been placed on a sound physical basis. In addition, experimental evidence has been presented regarding the finite growth time of gaseous-type cavitation bubbles and the variation of the cavitation threshold with the ambient hydrostatic pressure.

**CHAPTER VI****EPILOGUE**

This memorandum is based upon a study [55] completed at this laboratory. In this short epilogue some hindsight shall be exercised and speculations shall be made regarding possible work in the field of cavitation in liquids.

The study of the formation of cavitation bubbles by ultrasonic waves promises to be one of the best ways in which the phenomenon of cavitation and its relation to the theory of liquids can be examined. The number of variables that are involved in this study are so extensive that one could propose numerous experiments and problems. For example, the first question that one might ask is: What effect will the removal of all colloidal matter from a liquid have upon the cavitation process in the body of a liquid? The answer to this question can be obtained only by means of experimentation. Liquids can be "cleansed" by centrifuging, filtering, and/or other electrolytic techniques. Such liquids should be studied, although the design of the acoustic apparatus for the generation of very intense sound waves may prove difficult.

A second question that one is tempted to ask is: What is the actual growth curve of a gas-filled bubble into which there is a net diffusion of gas (sonically-induced)? It appears that the answer to this question will require further experimental and theoretical work. Perhaps high speed motion pictures can be used to obtain these data. Or one might be able to construct

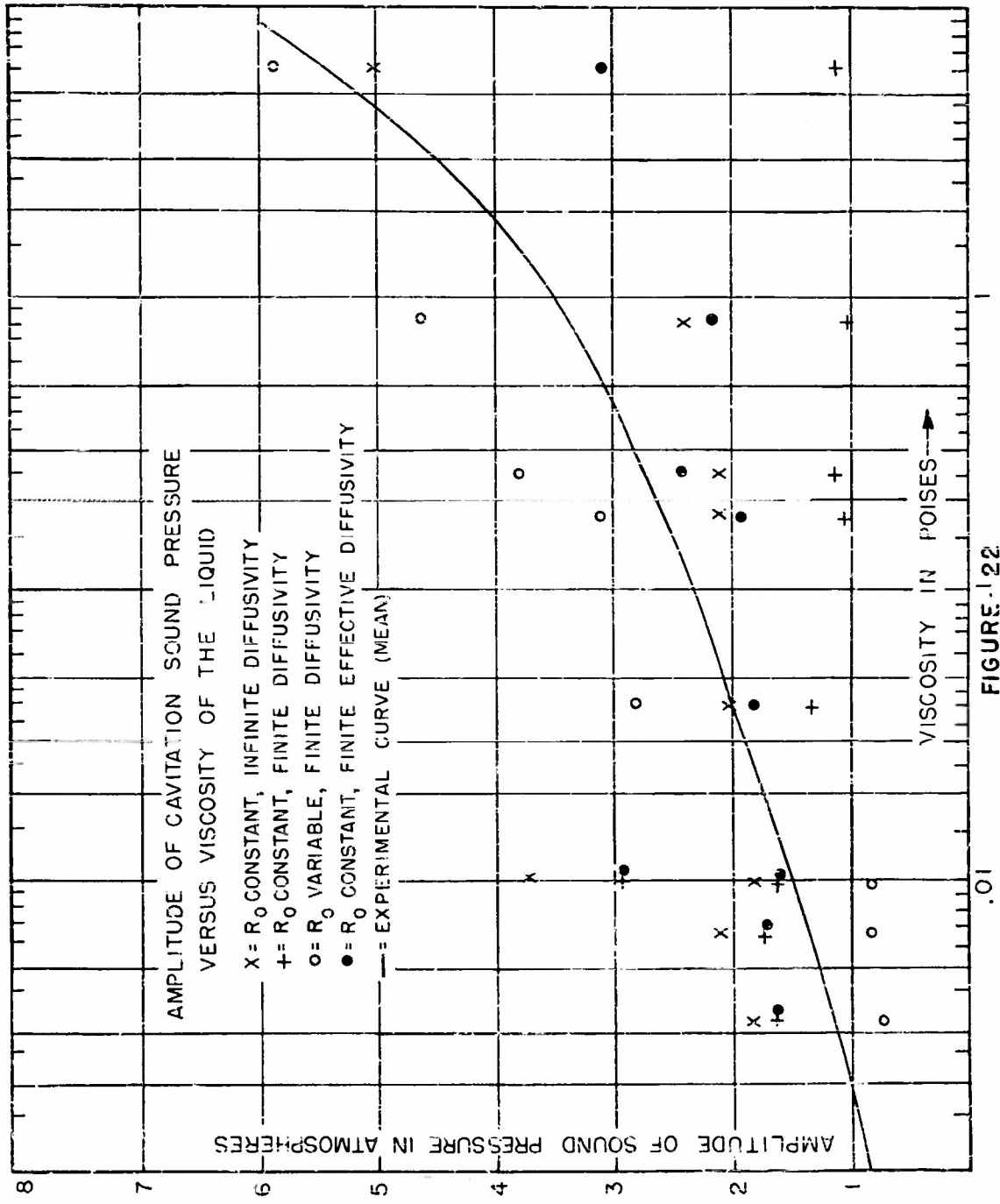


FIGURE 1.22

a cell in which a liquid can be observed microscopically while subject to ir-radiation by an acoustical signal. The theoretical analysis of this problem will probably result in a description of the time dependence of the radius of the bubble in terms of an equation that will require numerical integration. However, the data that are obtained would indicate the relative importance of several effects during the growth of the bubble.

Similar questions regarding the growth and collapse of vaporous-type bubbles must be answered. Phenomena associated with this growth and collapse should be studied, such as the luminescence effect observed in liquids undergoing intense cavitation. This effect is currently being ob-served and measured at this laboratory, and the experimental results will be presented, if possible, in a later memorandum.

Several other problems can be suggested, such as the importance of the frequency of the applied sound wave, or the importance of the type of gas within the liquid undergoing cavitation. It is indeed apparent that the study of sonic cavitation still presents many interesting and important problems.

#### Acknowledgment

The author wishes to express his gratitude to Professor F. V. Hunt, director of the Acoustics Research Laboratory, for his assistance in this study.

Supplement

During the period that this memorandum has been in print several additional articles regarding gaseous-type cavitation have appeared in the literature. Considerable experimental evidence has been accumulated by Lauer [56], Exner [57], and Exner and Hampe [58] to show that the damping of pulsating air bubbles in water can be explained in terms of the energy losses resulting from heat conduction and sound radiation. The damping due to viscosity appeared to be considerably smaller than would be expected from theory. In addition, Exner and Hampe [58] found that in the frequency range of their study (100 kc/s) the association of dust particles at the surface of the bubble resulted in a resonant frequency rise. The authors offer no explanation for this rise in frequency. Strassberg [59] has shown that the resonant frequency will increase slightly if the bubble becomes spheroidal, or if a free surface is nearby, but that the resonant frequency will decrease if a rigid surface is nearby. Binnie [60] has shown that for most cases the surface tension will provide sufficient stabilization to maintain the stability of the bubble's surface. However, the pressure of foreign particles probably can lead to instability, and a bubble that is wildly resonating in a sound field of appreciable intensity satisfies none of the assumptions upon which the above analyses are based. The analysis of the resonant bubble undergoing large excursions still requires study.

The noise produced by pulsating bubbles has received recent attention by Lange [61] and Harrison [62], with reference to its detection as an indication of cavitation and the transient pressure pulse associated with a collapsing bubble.

Pode [63] has extended the study of the growth in a sound field of bubbles with dimensions smaller than their resonant size. By using a perturbation technique he has considered the importance of the changes in bubble dimensions that are quadratically dependent upon pressure. In addition he has considered in the diffusion equation the convection term resulting from the pulsations of the bubble. Plesset and Zwick [64] by a method of successive approximations also have considered

the effect of a moving boundary on a similar problem.

Two elaborate experimental studies of cavitation have been presented by Willard [ 65] and Galloway [ 66]. Derouet [ 67] has written a short note regarding the degassing of liquids by sound waves. Willard made use of the streaming effect at the focus of a sound focusing system and obtained high speed photographs of the manner in which cavitation bubbles grow. He describes a step-by-step process for the growth of the non-collapsing gaseous-type and collapsing vaporous-type cavitation bubbles, both of which require the same initiation phases. Galloway has used a resonant glass sphere filled with liquid. By means of this system he has been able to obtain high acoustic pressures at the center of the sphere and precise measurements as to the variation of cavitation threshold with several parameters such as gas content, temperature, hydrostatic pressure, and type of liquid. Both of the above authors include extensive bibliographies.

## BIBLIOGRAPHY

- [1] PARSONS, C. A. and COOK, S. S., "Investigations into the Causes of Corrosion or Erosion of Propellers," Engineering 107, 515 (1919).
- [2] WISLICENUS, G. F., Fluid Mechanics of Turbomachinery, McGraw-Hill, New York, 1947.
- [3] BLAKE, F. G., Jr., "The Onset of Cavitation in Liquids," Doctoral Thesis, Harvard University, Cambridge, Massachusetts, January 1949.
- [4] EISENBERG, P., "On the Mechanism and Prevention of Cavitation," David Taylor Model Basin Report 712, July 1950.
- [5] SCHNEIDER, A. J. R., "Some Compressibility Effects in Cavitation Bubble Dynamics," Doctoral Thesis, California Institute of Technology, Pasadena, California, 1949.
- [6] RICHARDS, W. T., "Supersonic Phenomena," Rev. Mod. Phys. 2, 36 (1939).
- [7] BERGMANN, L., Der Ultraschall und seine Anwendung in Wissenschaft und Technik, Hirzel, Zurich, 1949.
- [8] RAVEN, F. A., FEILER, A. M., and JESPERSEN, A., "An Annotated Bibliography of Cavitation," David Taylor Model Basin Report R-81, December 1947.
- [9] BRIGGS, H. B., JOHNSON, J. B., and MASON, W. P., "Properties of Liquids at High Sound Pressures," J. Acoust. Soc. 19, 664 (1947).
- [10] TEMPERLEY, H. N. V., and CHAMBERS, L. L. G., "The Behavior of Water under Hydrostatic Tension," Proc. Phys. Soc. (London), Part I: 58, 420 (1946); Part II: 58, 436 (1946); Part III: 59, 199 (1947).
- [11] BENSON, S. W., and GERJUOY, E., "The Tensile Strength of Liquids. I. Thermodynamic Considerations," J. Chem. Phys. 17, 914 (1949).
- [12] DORING, W., "Die Überhitzungsgrenze und Zerreissfestigkeit von Flüssigkeiten," Z. Physik. Chem. B 36, 371 (1938); correction: Z. Physik. Chem. B 38, 292 (1939).
- [13] VOLMER, M., Kinetik der Phasenbildung, Theodor Steinkopff, Dresden und Leipzig, 1939.
- [14] FISHER, J. C., "The Fracture of Liquids," J. Appl. Phys. 19, 1062 (1948).
- [15] TURNBULL, D., and FISHER, J. C., "Rate of Nucleation in Condensed Systems," J. Chem. Phys. 17, 71 (1949).
- [16] FRENKEL, J., Kinetic Theory of Liquids, Oxford, 1946.
- [17] BORN, M., and GREEN, H. S., A General Kinetic Theory of Liquids, Cambridge, 1949.

- [ 18] GURNEY, R. W., Introduction to Statistical Mechanics, McGraw-Hill, New York, 1949.
- [ 19] TOLMAN, R. C., The Principles of Statistical Mechanics, Oxford, 1938.
- [ 20] DEAN, R. B., "The Formation of Bubbles," J. Appl. Phys. 15, 446 (1944).
- [ 21] CASSEL, H. M., "Physical Aspects of Foaming in Steam Generation," J. Appl. Phys. 15, 792 (1944).
- [ 22] HARVEY, E. N., COOPER, K. W., and WHITELEY, A. H., "Bubble Formation from Contact of Surfaces," J. Am. Chem. Soc. 68, 2119 (1946).
- [ 23] BIKERMAN, J. J., Surface Chemistry for Industrial Research, Academic Press, New York, 1948.
- [ 24] HARVEY, E. N., WHITELEY, A. H., McELROY, W. D., PEASE, D. C., and BARNES, D. K., J. Cell. and Comp. Physiology 24, 23. (1944).
- [ 25] HARVEY, E. N., McELROY, W. D., and WHITELEY, A. H., J. Appl. Phys. 18, 162 (1947).
- [ 26] DALLA VALLA, J. M., Micromeritics, Pitman, New York, 1948.
- [ 27] ROSENBERG, M. D., Technical Memorandum No. 25, Acoustics Research Laboratory, Harvard University, August 8, 1952.
- [ 28] HARVEY, E. N., BARNES, D. K., McELROY, W. D., WHITELEY, A. H., and PEASE, D. C., "Removal of Gas Nuclei from Liquids and Surfaces," J. Am. Chem. Soc. 67, 156 (1945).
- [ 29] POISEUILLE, J. L. M., "Recherches Experimentales sur le Mouvement des Liquides dans les Tubes de Tres Petits Diametres," Comptes rendus 11, 961 (1840); 12, 112 (1841); Mem. des Sav. Etrangers 2, 433 (1846).
- [ 30] LAMB, H., Hydrodynamics, Dover, New York, 1945.
- [ 31] ZSIGMONDY, R. A., Colloids and the Ultramicroscope, Wiley, New York, 1909.
- [ 32] SHILLABER, C. P., Photomicrography, Wiley, New York, 1944.
- [ 33] PEKERIS, C. L., "The Rate of Rise and Diffusion of Air Bubbles in Water," NDRC Report No. C4-srZ0-326, 1942.
- [ 34] LORD RAYLEIGH, "On the Superficial Viscosity of Water," Proc. Roy. Soc. (London) XLVIII, 127 (1890).
- [ 35] STEWART, G. W., and LINDSAY, R. B., Acoustics, D. Van Nostrand, New York, 1930.
- [ 36] KINSLER, L. E., and FREY, A. R., Fundamentals of Acoustics, Wiley, New York, 1950.

- [ 37] BORN, M., Optik, Verlag. Julius Springer, Berlin, 1933.
- [ 38] PRESTON, T., The Theory of Light, Macmillan, London, 1928.
- [ 39] GRIFFING, V., and FOX, F.E., "Theory of Ultrasonic Intensity Gain due to Concave Reflectors," J. Acoust. Soc. 21, 348 (1949).
- [ 40] ROCARD, Y., Dynamique Generale des Vibrations, Masson, Paris, 1949.
- [ 41] GERNEZ, M., "Sur le Degagement des Gaz de Leurs Solutions Sursaturees," Comptes rendus 63, 883 (1866).
- [ 42] KENRICK, F.E., WISMER, K.L., and WYATT, K.S., "Supersaturation of Gases in Liquids," J. Phys. Chem. 28, 1308 (1924).
- [ 43] METSCHL, J., "The Supersaturation of Gases in Water and Certain Organic Liquids," J. Phys. Chem. 28, 417 (1924).
- [ 44] SCHWEITZER, P.H., and SZEBEHELY, V.G., "Gas Evolution in Liquids and Cavitation," J. Appl. Phys. 21, 1218 (1950).
- [ 45] SZEBEHELY, V.G., "Relation between Gas Evolution and Physical Properties of Liquids," J. Appl. Phys. 22, 627 (1951).
- [ 46] BJERKNES, V.F.K., Fields of Force, Columbia University Press, New York, 1906.
- [ 47] BJERKNES, V.F.K., Die Kraftfelder, Friedrich Vieweg und Sohn, Braunschweig, 1909.
- [ 48] BASSET, A.B., A Treatise on Hydrodynamics, Vol. I, Cambridge, 1888, p. 255.
- [ 49] WESTERVELT, P.J., "The Mean Pressure and Velocity in a Plane Acoustic Wave in a Gas," J. Acoust. Soc. 22, 319 (1950).
- [ 50] WESTERVELT, P.J., "The Theory of Steady Forces Caused by Sound Waves," J. Acoust. Soc. 23, 312 (1951).
- [ 51] ECKART, C., "Vortices and Streams Caused by Sound Waves," Phys. Rev. 73, 68 (1948).
- [ 52] ARNOLD, J.H., "Studies in Diffusion. I. Estimation of Diffusivities in Gaseous Systems," Ind. Eng. Chem. 22, 1091 (1930).
- [ 53] ARNOLD, J.H., "Studies in Diffusion. II. A Kinetic Theory of Diffusion in Liquid Systems," J. Am. Chem. Soc. 52, 3937 (1930).
- [ 54] PARTINGTON, J.R., An Advanced Treatise on Physical Chemistry, Vol. I, "The Properties of Gases," Longmans, 1949; Vol. II, "The Properties of Liquids," Longmans, 1951.
- [ 55] ROSENBERG, M.D., "Gaseous-Type Cavitation in Liquids," Doctoral Thesis, Harvard University, Cambridge, Massachusetts, 1952.

- [ 56] LAUER, H., "Über Die Thermische Dämpfung von Blasen Verschiedener Gase in Wasser," Akustische Beihefte 1, 12 (1951).
- [ 57] EXNER, M. L., "Messung der Dämpfung Pulsierender Lufblasen in Wasser," Akustische Beihefte 1, 25 (1951).
- [ 58] EXNER, M. L., and HAMPE, W., "Experimental Determination of the Damping of Pulsating Air Bubbles in Water," Acustica, 3, 67 (1953).
- [ 59] STRASBERG, M., "Pulsation Frequency of Non-spherical Gas Bubbles in Liquids," J. Acoust. Soc. Am., 25, 536 (1953).
- [ 60] BINNIE, A. M., "The Stability of the Surface of a Cavitation Bubble," Proc. Camb. Phil. Soc. 49, 151 (1953).
- [ 61] LANGE, T., "Methoden zur Untersuchung der Schwingungskavitation in Flüssigkeiten mit Ultraschall," Akustische Beihefte 2, 75 (1952).
- [ 62] HARRISON, M., "An Experimental Study of Single Bubble Cavitation Noise," J. Acoust. Soc. Am., 24, 776 (1952).
- [ 63] PODE, L., "The Deaeration of Water by a Sound Beam, David Taylor Model Basin Report No. 854, May 1953, Washington, D. C.
- [ 64] PLESSET and ZWICK, "A Non-steady Heat Diffusion Problem with Spherical Symmetry," J. Appl. Phys. 23, 95 (1952).
- [ 65] WILLARD, G. W., "Ultrasonically Induced Cavitation in Water: A Step-by-step Process," J. Acoust. Soc. Am. 25, 669 (1953).
- [ 66] GALLOWAY, W. J., An Experimental Study of Acoustically Induced Cavitation, Dept. of Physics, Univ. of Calif., Los Angeles, Tech. Report No. VII, November 1953.
- [ 67] DERROQUET, B., "Etude du degazage des liquides sous l'effect des vibrations ultraanores à 80 et 17.7 Kc/s," Comptes Rendus Acad. Sci. (Paris) 234, 71 (1952).

**Project X**

**Distribution**

1                   **Research and Development Board**  
                      **Pentagon Building**  
                      **Washington 25, D. C.**

2                   **Chief of Naval Research**  
                      **Attn: Acoustics Branch, Code 411**  
                      **Office of Naval Research**  
                      **Washington 25, D. C.**

1                   **Director**  
                      **Naval Research Laboratory**  
                      **Washington 25, D. C.**  
                      **Attn: Technical Information Officer**

**Commanding Officer**  
                      **U. S. Navy Office of Naval Research**  
                     **Branch Offices:**

1                   **Boston**  
1                   **New York**  
1                   **Chicago**  
1                   **Pasadena**

3                   **Officer in Charge**  
                     **Office of Naval Research**  
                     **Navy No. 100, Fleet Post Office**  
                     **New York, New York**

1                   **Director**  
                     **U. S. Navy Underwater Sound**  
                     **Reference Laboratory**  
                     **Office of Naval Research**  
                     **Orlando, Florida**

1                   **Director**  
                     **Naval Research Laboratory**  
                     **Sound Division**  
                     **Washington 20, D. C.**

1                   **Director**  
                     **U. S. Naval Electronics Laboratory**  
                     **San Diego 52, California**

1                   **U. S. Naval Academy**  
                     **Naval Postgraduate School**  
                     **Physics Department**  
                     **Monterey, California**  
                     **Attn: Prof. L. E. Kinsler**

1 Director  
Naval Ordnance Laboratory  
White Oaks, Maryland  
Attn: Sound Division

1 Director  
Marine Physical Laboratory  
University of California  
U. S. Navy Electronics Laboratory  
San Diego 52, California

1 Director  
U. S. Navy Underwater Sound Laboratory  
Fort Trumbull  
New London, Connecticut

1 Director  
David Taylor Model Basin  
Carderock, Maryland  
Attn: Sound Section

1 Director  
Ordnance Research Laboratory  
Pennsylvania State College  
State College, Pennsylvania

Navy Department  
Bureau of Ships  
Washington 25, D. C.  
Attn: Code 847  
845  
665E

1 Naval Medical Research Institute  
Naval Medical Center  
Bethesda, Maryland  
Attn: LCDR D. Goldman, NMC

1 U. S. Undersea Warfare Committee  
Navy Department  
Washington 25, D. C.

1 Massachusetts Institute of Technology  
Acoustics Laboratory  
Cambridge 38, Massachusetts  
Attn: Professor R. H. Bolt

1 Catholic University of America  
Washington 17, D. C.  
Attn: Professor K. F. Herzfeld,

1 Brown University  
Department of Applied Physics  
Providence 12, Rhode Island  
Attn: Professor R. B. Lindsay

1 University of California  
Department of Physics  
Los Angeles, California

1 Princeton University  
Department of Electrical Engineering  
Princeton, New Jersey

1 Utah University  
Salt Lake City 1, Utah  
Attn: Dr. P. J. Elsey

1 Western Reserve University  
Department of Chemistry  
Cleveland, Ohio  
Attn: Dr. Ernest Yeager

1 Commanding Officer  
Naval Air Development Center  
Johnsville, Pennsylvania

1 Woods Hole Oceanographic Institute  
Woods Hole, Massachusetts  
Attn: Mr. Vine

1 National Bureau of Standards  
Sound Section  
Washington 25, D. C.

1 California Institute of Technology  
Pasadena, California  
Attn: Dr. Epstein

1 Commanding Officer  
Air Force Cambridge Research Laboratory  
230 Albany Street  
Cambridge 39, Massachusetts

1 Los Alamos Scientific Laboratory  
P. O. Box 1663  
Los Alamos, New Mexico  
Attn: Dr. G. L. Campbell

Project X

-4-

1 Case Institute of Technology  
Department of Physics  
University Circle  
Cleveland 6, Ohio  
Attn: R. S. Shankland

1 California Institute of Technology  
Department of Chemical Engineering  
Pasadena, California  
Attn: Dr. M. S. Plesset

1 Department of Electrical Engineering  
U. S. Naval Academy  
Annapolis, Maryland

1 Lois A. Noble, Librarian  
The Brush Development Company  
3405 Perkins Avenue  
Cleveland 14, Ohio

1 Kellex Corporation  
Silver Spring Laboratory  
Silver Spring, Maryland

1 Technical Library  
Bell Telephone Laboratories  
Murray Hill, New Jersey

1 National Academy of Sciences  
Committee on Undersea Warfare  
2101 Constitution Avenue  
Washington 25, D. C.  
Attn: Dr. John S. Coleman

1 Commanding Officer:  
U. S. Naval Ordnance Test Station  
Inyokern, California  
Attn: Reports Unit